NASA TECHNICAL NOTE

NASA TN D-4376

C 1

TECH LIBRARY KAFB, NM
0131455

NASA TN D-4376

LOAN COPY: RETURN TO
AFWL (WLIL-2)
KIRTLAND AFB, N MEX

COLLISIONLESS SHEATHS BETWEEN FIELD-MODIFIED EMITTERS AND THERMALLY IONIZED PLASMAS EXEMPLIFIED BY CESIUM

by James F. Morris

Lewis Research Center

Cleveland, Ohio

NATIONAL AERONAUTICS AND SPACE ADMINISTRATION • WASHINGTON, D. C. • AUGUST 1968

TECH LIBRARY KAFB, NM
0131455
NASA TN D-4376

COLLISIONLESS SHEATHS BETWEEN FIELD-MODIFIED EMITTERS AND THERMALLY IONIZED PLASMAS EXEMPLIFIED BY CESIUM

By James F. Morris

Lewis Research Center
Cleveland, Ohio

NATIONAL AERONAUTICS AND SPACE ADMINISTRATION

For sale by the Clearinghouse for Federal Scientific and Technical Information
Springfield, Virginia 22151 – CFSTI price $3.00

COLLISIONLESS SHEATHS BETWEEN FIELD-MODIFIED EMITTER AND THERMALLY IONIZED PLASMA EXEMPLIFIED BY CESIUM

by James F. Morris

Lewis Research Center

SUMMARY

This report gives a model, an iterative calculation method, and results for plane collisionless sheaths. These sheaths separate thermally ionized plasmas (Saha) from emitters of electrons (Richardson-Dushman), ions, and atoms (Saha-Langmuir) and change emission with their fields (Schottky). Still the model gives identical absolute potential changes through the sheath for ions and electrons, contrary to usual practice. For cesium, the emitter and plasma ion and atom temperatures range from 1600° to 2400° K with plasma electron temperatures up to 300° K higher. Plasma electron number densities are 10^{12} to 10^{15} per cubic centimeter. At these conditions work functions from 1.5 to 5 volts produce absolute potential drops from 0 to 1.5 volts for electron and positive-ion sheaths. And some currents greater than 10^{2} amperes per square centimeter result.

For this study certain generalizations apply: Sheath fields affect emissions and sheath characteristics significantly. The overall sheath characteristics correlate better with an emission Debye length (6.9 times the square root of the emitter temperature ($^{\circ}$K) divided by the plasma electron number density (cm^{-3})) than with the conventional Debye length. Where conditions comply with the assumptions of the model, effective sheath widths decrease from 2.6 to 2 emission Debye lengths as overall sheath drops grow from less than 0.1 to 1.5 volts.

INTRODUCTION

In gaseous electronics an electrode exchanges flows of electrons, ions, and atoms with an ionized gas. Depending on the properties of the system, the potential of the solid surface generally runs above or below that of the plasma. The region between the plasma and the emitter builds up an excess of electrons or positive ions. Under certain

conditions these sheaths submit to analyses based on existing theories. For example, relations for equilibrium ionization, emission, acceleration, and potential combine to form a simple picture of a collisionless adaptive region between an electrode and an ionized gas. This sheath model with its iterative calculation method and some results for cesium make up the present report.

Although a sheath and a net current generally attend an emitter in gaseous electronics, they vanish at a special state of equilibrium, the Saha-Langmuir null point (ref. 1). Here the emitter injects electrons, ions, and atoms into the plasma at rates that exactly balance the departures of these particles from the equilibriated thermally ionized gas. In other words, the Richardson-Dushman emission of electrons (refs. 2 to 4) and the Saha-Langmuir emissions of ions and atoms (ref. 1) equal the respective random particle currents to the emitter from the Saha plasma (ref. 5). With the ionization potential, pressure, and matched plasma and electrode temperatures all fixed, equilibrium dictates the work function at the Saha-Langmuir null point.

If the work function is less than the value that yields no net current or sheath, fewer positive ions and more electrons escape the emitter. Then an excess of negative charge gathers near the face of the metal and diminishes toward neutrality in the plasma, forming an electron sheath. When the work function is greater than that of the Saha-Langmuir null point, emission increases for ions and decreases for electrons. Now a surplus of positive charge collects at the solid surface and diminishes toward zero in the plasma, producing an ion sheath. In both positive-ion and electron sheaths, though, no net currents result if the emitter remains at the temperature of the equilibrium plasma.

But sheaths sometimes confront electrode surfaces with great charge concentrations and high fields that create problems not anticipated in the Saha-Langmuir model. And if the system is not isothermal, if net charge flows, if conditions depart from equilibrium in any way, both the Saha-Langmuir and Saha theories fail - technically. Practically, however, these relations serve well for many nonequilibrium conditions (refs. 6 to 8). For certain modes of operation the Saha and Saha-Langmuir equations adequately describe power producing thermal-plasma devices like thermionic converters (refs. 6 to 9).

Because electrodes as well as plasmas contribute charged particles in the thermionic diode, both of these active elements affect charge concentrations in the sheaths of this energy converter. Although many previous studies analyzed sheath problems (refs. 9 to 27), those that dealt with plasmas and probes used nonemitting or nonionizing electrodes. And those that treated emitters included no ionization mechanism within the plasma and no increases in emission caused by the effective lowering of the work function by electric fields (ref. 28, Schottky).

These Schottky depressions of potential barriers at emitters often affect charge transport greatly in thermionic diodes. For example, a 1-volt sheath of a plasma with

10^{14} electrons per cubic centimeter at 3000^{o} K probably rises about 10^{4} volts per centimeter near the electrode. This field cuts almost 0.04 volt from the effective work function and frees 25 percent more electrons than escape with no field. Such reduced barrier potentials and increased emission currents demonstrate that sheath models for thermionic diodes need Schottky modifications.

This work describes a field-corrected emitter (Richardson-Dushman, Saha-Langmuir, Schottky) connected through a collisionless sheath (electron or positive-ion) to a thermally ionized plasma (Saha). The sheath produces identical overall changes in absolute potential for electrons and ions, contrary to the results of usual Schottky analyses. To illustrate the present model, plots and tables in this report give charge and current densities, electric fields and potentials, and widths of sheaths for cesium plasmas. Electrode, ion, and atom temperatures range from 1600^{o} to 2400^{o} K; electron temperature varies from 1700^{o} to 2700^{o} K; work function runs from 1.5 to 5.0 volts; and electron number density goes from 10^{12} to 10^{15} per cubic centimeter.

The results presented reflect the restrictions of the model: The sheath is essentially collisionless. Emitter, ion, atom, and plasma temperatures are similar. Net currents are small compared with random circulations. And the plasma pressures for cesium are below its vapor pressures at the electrode temperatures.

These computations convert to another plasma merely by replacing the minimum mean free path, vapor pressure, and ionization potential of cesium with those of the desired element.

THEORY

As stated in the INTRODUCTION, this model joins a thermally ionized plasma to a field-corrected emitter with a collisionless sheath. The theory begins, however, with the exact Saha-Langmuir solution that yields no sheath and no net current.

SAHA-LANGMUIR NULL POINT

The plasma model synthesized for the present analysis contains only electrons and singly ionized and ground-state atoms. This simple model serves well for low temperatures. In equilibrated cesium plasmas, for example, excited atoms are an appreciable part of the neutrals only above 3000^{o} K. At equilibrium, the proposed composition follows Saha's expression for the law of mass action:

$$N_{e,P} = \frac{N_{a,P}}{N_{i,P}} \left(\frac{2\pi m_e \kappa T_{e,P}}{h^2} \right)^{3/2} \exp\left(- \frac{eI}{\kappa T_{e,P}} \right) \tag{1}$$

Because these plasma electrons (eq. (1)) form a Maxwellian distribution, one-half of them moves in any one direction with the average velocity $(2\kappa T_{e,P}/\pi m_e)^{1/2}$ at any given time. A random current density results:

$$j_{e,P} = \left(\frac{2\kappa T_{e,P}}{\pi m_e} \right)^{1/2} \frac{N_{e,P} e}{2} = \frac{4\pi m_e (\kappa T_{e,P})^2 e}{2h^3} \left(\frac{N_{a,P}}{N_{i,P}} \right) \exp\left(- \frac{eI}{\kappa T_{e,P}} \right) \tag{2}$$

When this flow cancels the electron emission from a surface at the plasma temperature, the electrode and the ionized gas equilibrate:

$$j_{e,E} = \frac{4\pi m_e (\kappa T_E)^2 e}{h^3} \exp\left(- \frac{e\varphi}{\kappa T_E} \right) = \frac{4\pi m_e (\kappa T_{e,P})^2 e}{2h^3} \left(\frac{N_{a,P}}{N_{i,P}} \right) \exp\left(- \frac{eI}{\kappa T_{e,P}} \right) = j_{e,P}$$

or

$$\frac{N_{i,P}}{N_{a,P}} = \frac{\exp\left[\frac{e(\varphi - I)}{\kappa T_E} \right]}{2} = \frac{N_{i,E}}{N_{a,E}} = \frac{j_{i,E}}{j_{a,E}} \tag{3}$$

With its denominator of 2, the Saha-Langmuir relation (eq. (3)) applies when the statistic weight of the ion is one-half that of the atom. This situation occurs in ground-state, singly ionized alkali-metal vapors. Here the emissions described by equation (3) exactly replace ion and atom losses from the ionized gas. Because no sheath intervenes, a given plasma demands one particular work function for true equilibrium with an electrode. Work functions that produce these Saha-Langmuir null points for some cesium plasmas appear in figure 1.

SHEATHS

Generally, the work function of the emitter fails to satisfy the requirements for a Saha-Langmuir null point. Then a sheath adapts the plasma to the electrode and equalizes the countercurrents in the isothermal system. Sheaths usually occur in heterothermal combinations of emitters and ionized gases also. But, in the strictest sense, the present development applies only where all temperatures are alike.

For these calculations charge balance and zero electric field prevail in the bulk ionized gas. Zero reasonably approximates the fields needed for the comparatively small current densities in the plasma. As the distance from the electrode increases, the sheath conditions approach those of the plasma. In practice, though, various particle and group interactions preclude this asymptote, and much of the sheath potential drop occupies a relatively small distance. This rationale leads to the concept of an effective sheath width with an approximate charge balance at the plasma boundary. Further discussion later will clarify this idea.

Virtual Schottky Emitter

The present study analyzes a sheath attached to an electrode that emits electrons, ions, and atoms. The sheath lowers the emission barrier for the charge it accelerates and frees more accelerated particles than escape from a sheathless emitter. A positive-ion sheath releases more electrons; an electron sheath looses more positive ions. Consideration of this effect led to the use of a new electrode model called a virtual Schottky emitter. On its surface, particle potentials differ in absolute value from those in the plasma by the sheath drop for the accelerated charge. But this is a deceptively simple definition. Perhaps the virtual Schottky emitter requires additional explanation, beginning with a description of traditional theoretic thermionic emission.

Without external fields, an electron converts kinetic energy to potential while leaving a conductor. The total energy change for an exodic electron equals the work function of the emitter. Schottky suggested that the electron works against the attraction of its mirror image to escape. The electron and its image are equally but oppositely distant from the conductor surface. As a result, the charge pair attract each other with a force inversely proportional to four times the square of the distance of the electron from the emitter, $e^2/4x^2$. Of course this force has no meaning at the surface. Furthermore, the image effect applies only for a single charged particle departing from the plane face of a conductor, precluding other particles and external fields. But experiments verify image forces in the presence of other particles and of external fields (ref. 6).

Thus, when an electron moves toward a conductor from very far away, it loses po-

tential energy equal to the image force times its distance from the surface, $e^2/4x$. Because this change lowers the free-space potential energy of the electron, it subtracts from the work function, $e\varphi - e^2/4x$. Dividing this potential energy by the electronic charge yields the motive, which figure 2(a) shows. The mirror image effect requires the use of the motive concept because in this situation the usual definition of potential has no meaning.

If a charged particle moves in superposed electrostatic fields, its charge divided into the potential energy resulting from the mirror image and all external fields is its motive. But here, as throughout thermionics, "potential" is also used to mean "motive." The negative gradient of any motive equals the electrostatic force on the particle divided by its charge. A particle field of this type results from the mirror image, $e/4x^2$.

When an external field acts on an emitter, it adds vectorially to the image force. With a constant applied field that accelerates electrons, the emission motives become $\varphi - (e/4x) - Ex$ for the electrons and $\varphi - (e/4x) + Ex$ for the ions; these functions appear in figure 2(b). On the lower curve the maximum $\varphi - (eE)^{1/2}$ occurs at a distance $e/2(eE)^{1/2}$ from the conductor surface. This depression of the emission barrier, effectively reducing the work function for the electron, is the Schottky effect.

If the applied field accelerates the positive ion, the upper curve of figure 2(b) describes the electronic potential. Then, as the lower curve indicates, the emission barrier for positive ions decreases.

Traditionally, thermionics treats the work function and the Schottky effect as surface, not space, phenomena. This assumption leads to motives that terminate at the emitter face like those in figure 2(c). In the present model the electron and ion potentials in the plasma lie at equal displacements above and below the origin. For usual analyses, though, emission barriers are the work function for the ion and the field-corrected work function for the electron. When the plasma potentials subtract from those at the emitter, the ion-sheath drops become $\varphi_0 - \varphi$ for ions and $\varphi - \varphi_0 - (eE_E)^{1/2}$ for electrons. Thus, particles with equal but opposite charges undergo different absolute potential changes while passing through the same sheath. Furthermore, the traditional emitter of figure 2(c) produces net currents through the sheath in an isothermal system. Obviously then, the usual thermionic model fails in a sheath analysis.

A motive like that of figure 2(b) seems necessary to combine the image and sheath potentials, as the diagrams of figure 2(d) show. For these motives no net charge flows when all temperatures are alike. But now the emission mechanism fuses complexly and inseparably with the sheath transport mechanism, preventing good independent estimates of emitter characteristics. The transition region looks like a single sheath for one charge and a double sheath for the other, with the image potential extending through the

sheath and the plasma. This means that plasma calculations include effects of surface potentials for all electrodes and containers.

The extension of the image potential through the sheath and the plasma, however, lacks both theoretic and experimental support. As reference 9 puts it, ". . . the mirror-image force is of little or no consequence at a distance from the conducting surface of 10^{-8} meter . . . ." Because the superposition of figure 2(d) is unreal and complicated, it seems a poor replacement for the traditional model of figure 2(c), which is incorrect but simple.

Thermionics needs an effective emitter that separates emission from sheath and plasma processes yet submits to the second law of thermodynamics. The virtual Schottky emitter offers the compromise shown in figure 2(e). In this model, electrons and positive ions pass through the same absolute potential change across the sheath, $\Delta V_o - (eE_E)^{1/2}$ for the ion sheath and $\Delta V_o - (-eE_E)^{1/2}$ for the electron sheath. Simultaneous emissions of electrons, ions, and atoms encounter the same effective work functions, $\varphi - (eE_E)^{1/2}$ for the ion sheath and $\varphi + (-eE_E)^{1/2}$ for the electron sheath. The sheath potentials for ions and electrons at the emitter occur at slightly different distances from the solid surface. But all of the other emission models for electrodes in plasmas also have this problem. Finally, no net charge flows for isothermal systems involving virtual Schottky emitter.

The virtual Schottky emitter, a theoretic construct that works for sheath calculations, is the basis of the present analysis.

Parameters

Calculations for both the positive-ion and electron sheaths begin with the specification of certain variables: emitter work function and temperature T_E; plasma electron, ion, and atom temperatures $T_{e,P}$, $T_{i,P}$, and $T_{a,P}$; plasma electron (and ion) number density $N_{e,P} = N_{i,P}$; and the ionization potential I, minimum mean free path λ, and vapor pressure at the electrode temperature (for a maximum arrival rate) p_{vp} for the plasma chemical. Values of these variables selected for the present solutions for cesium were

$$\varphi = 1.5 \text{ to } 5 \text{ V}$$

$$T_E = T_{i,P} = T_{a,P} = 1600^{\circ},\ 2000^{\circ},\ 2400^{\circ} \text{ K}$$

$$T_{e,P}(\geq T_{i,P}) = 1700^{\circ} \text{ to } 2700^{\circ} \text{ K}$$

$$N_{e,P} = 10^{12},\ 10^{13},\ 10^{14},\ 10^{15}\ cm^{-3}$$

$$I = 3.898\ V$$

$$\lambda = 0\left(10^{12}N_{a,P}^{-1}\right)cm \qquad \text{(ref. 29)}$$

$$p_{vp} = \frac{\text{anti}\log_{10}\left(+10.71914 - 0.51978\log_{10}T_E - 3920.38/T_E\right)}{133.322}\ torr \qquad \text{(ref. 30)}$$

Current Densities

A complete set of parameters leads ultimately to the determination of sheath fields and potentials from charge densities contributed by the currents. Random circulations within the plasmas come directly from the selected values of the variables. Because sheath conditions influence the virtual Schottky emitter, though, current densities of emissions require iterative calculations. The equations used are presented in the following sections.

Positive-ion sheath. - The plasma random current densities for the electrons, ions, and atoms (equivalent random current density from the Saha eq. (1)) are, respectively,

$$j_{e,P} = e\frac{N_{e,P}}{2}\left(\frac{2\kappa T_{e,P}}{\pi m_e}\right)^{1/2} \tag{4}$$

$$j_{i,P} = e\frac{N_{e,P}}{2}\left(\frac{2\kappa T_{i,P}}{\pi m_i}\right)^{1/2} \tag{5}$$

$$j_{a,P} = \frac{eN_{e,P}^2}{2\left(\frac{2\pi m_e \kappa T_{e,P}}{h^2}\right)^{3/2}\exp\left(-\frac{eI}{\kappa T_{e,P}}\right)}\left(\frac{2\kappa T_{a,P}}{\pi m_a}\right)^{1/2} \tag{6}$$

The following electron, ion, and atom current densities for the virtual Schottky emitter derive from the field-corrected Richardson-Dushman and Saha-Langmuir equations. Although the expressions for electron emission need modification for fields only,

those for ion and atom emission require adjustments in the cesium arrival rates for the sheath drops. In addition to the flow of neutrals from the plasma, the total cesium supply to the emitter includes ion streams that the sheaths cut off or reflect. That this adaptation further complicates the Saha-Langmuir relation seems obvious from a comparison of equation (3) with equations (8), (9), (16), (17), (19), (20), (24), and (25). The current density equations are as follows:

$$j_{e,E} = 120T_E^2 \exp\left[-\frac{e\varphi - \left(e^3 E_E\right)^{1/2}}{\kappa T_E}\right] \tag{7}$$

$$j_{i,E} = \frac{j_{i,P} + j_{a,P}}{2\exp\left[\frac{e(I-\varphi) + \left(e^3 E_E\right)^{1/2}}{\kappa T_E}\right] + \exp\left(-\frac{e\Delta V_S}{\kappa T_E}\right)} \tag{8}$$

$$j_{a,E} = \frac{j_{i,P} + j_{a,P}}{1 + \frac{1}{2}\exp\left[-\frac{e(\Delta V_S + I - \varphi) + \left(e^3 E_E\right)^{1/2}}{\kappa T_E}\right]} \tag{9}$$

Ion sheaths yield the following electron, ion, and overall net current densities:

$$j_e = j_{e,E} - j_{e,P}\exp\left(-\frac{e\Delta V_S}{\kappa T_{e,P}}\right) \tag{10}$$

$$j_i = j_{i,P} - j_{i,E}\exp\left(-\frac{e\Delta V_S}{\kappa T_E}\right) \tag{11}$$

$$J = j_e + j_i \tag{12}$$

When all the temperatures are alike, the net current densities reduce to zero for electrons, ions, and atoms:

$$\frac{j_{e,E}}{j_{e,P}} = \exp\left(-\frac{e\Delta V_S}{\kappa T}\right) \tag{13}$$

$$\frac{j_{i,P}}{j_{i,E}} = \exp\left(-\frac{e\Delta V_S}{\kappa T}\right) \tag{14}$$

$$\frac{j_{a,E}}{j_{a,P}} = 1 \tag{15}$$

Then expressions for isothermal ionization ratios result:

$$\frac{j_{i,P}}{j_{a,P}} = \frac{1}{2}\exp\left[\frac{e(-\Delta V_S - I + \varphi) - \left(e^3 E_E\right)^{1/2}}{\kappa T}\right] \tag{16}$$

$$\frac{j_{i,E}}{j_{a,E}} = \frac{1}{2}\exp\left[\frac{e(-I + \varphi) - \left(e^3 E_E\right)^{1/2}}{\kappa T}\right] \tag{17}$$

Electron sheath. - Equations (4) to (6) give the random plasma current densities for the electron sheath as well as for the ion sheath.

But the current densities from the virtual Schottky emitter for electrons, ions, and atoms change:

$$j_{e,E} = 120\, T_E^2 \exp\left[-\frac{e\varphi + \left(-e^3 E_E\right)^{1/2}}{\kappa T_E}\right] \tag{18}$$

$$j_{i,E} = \frac{j_{a,P} + j_{i,P}\exp\left(\frac{e\Delta V_S}{\kappa T_{i,P}}\right)}{1 + 2\exp\left[\frac{e(I - \varphi) - \left(-e^3 E_E\right)^{1/2}}{\kappa T_E}\right]} \tag{19}$$

$$j_{a,E} = \frac{j_{a,P} + j_{i,P} \exp\left(\frac{e\Delta V_S}{\kappa T_{i,P}}\right)}{1 + \frac{1}{2} \exp\left[-\frac{e(I - \varphi) - \left(-e^3 E_E\right)^{1/2}}{\kappa T_E}\right]} \tag{20}$$

The electron, ion, and overall net current densities are

$$j_e = j_{e,E} \exp\left(\frac{e\Delta V_S}{\kappa T_E}\right) - j_{e,P} \tag{21}$$

$$j_i = j_{i,P} \exp\left(\frac{e\Delta V_S}{\kappa T_{i,P}}\right) - j_{i,E} \tag{22}$$

$$J = j_e + j_i \tag{23}$$

When all the temperatures are alike, equations (13), (14), and (15) apply for the electron, ion, and atom, respectively. New expressions for isothermal ionization ratios result, however:

$$\frac{j_{i,P}}{j_{a,P}} = \frac{1}{2} \exp\left[\frac{e(-\Delta V_S - I + \varphi) + \left(-e^3 E_E\right)^{1/2}}{\kappa T}\right] \tag{24}$$

$$\frac{j_{i,E}}{j_{a,E}} = \frac{1}{2} \exp\left[\frac{e(-I + \varphi) + \left(-e^3 E_E\right)^{1/2}}{\kappa T}\right] \tag{25}$$

Charge Densities

With the preceding current densities for the plasma and the virtual Schottky emitter, adding transmitted and reflected flows divided by appropriate average velocities yields

charge densities. The average velocities result from integrations of (1) a half-Maxwellian velocity distribution for the retarded particles, (2) a half-Maxwellian truncated at the potential rise to the top of the sheath for reflected flow, and (3) a half-Maxwellian displaced by the potential drop for the accelerated charges.

Positive-ion sheath (electron potentials are positive numbers.) -

$$\rho_{\Delta V} = \frac{j_{e,E}\left\{1 - \operatorname{erf}\left[\frac{e(\Delta V_S - \Delta V)}{\kappa T_E}\right]^{1/2}\right\}\exp\left[\frac{e(\Delta V_S - \Delta V)}{\kappa T_E}\right]}{\left(\frac{2\kappa T_E}{\pi m_e}\right)^{1/2}}$$

$$+ \frac{j_{e,P}\left\{1 + \operatorname{erf}\left[\frac{e(\Delta V_S - \Delta V)}{\kappa T_{e,P}}\right]^{1/2}\right\}\exp\left(-\frac{e\,\Delta V}{\kappa T_{e,P}}\right)}{\left(\frac{2\kappa T_{e,P}}{\pi m_e}\right)^{1/2}}$$

$$- \frac{j_{i,E}\left[1 + \operatorname{erf}\left(\frac{e\,\Delta V}{\kappa T_E}\right)^{1/2}\right]\exp\left[-\frac{e(\Delta V_S - \Delta V)}{\kappa T_E}\right]}{\left(\frac{2\kappa T_E}{\pi m_i}\right)^{1/2}}$$

$$- \frac{j_{i,P}\left[1 - \operatorname{erf}\left(\frac{e\,\Delta V}{\kappa T_{i,P}}\right)^{1/2}\right]\exp\left(\frac{e\,\Delta V}{\kappa T_{i,P}}\right)}{\left(\frac{2\kappa T_{i,P}}{\pi m_i}\right)^{1/2}} \qquad (26)$$

The two positive terms give the electron charge density at ΔV while the two negative terms represent the ions. In the plasma, $\Delta V = 0$ and equation (26) becomes

$$\rho_P = 0 = \frac{j_{e,E}\left[1 - \operatorname{erf}\left(\frac{e\,\Delta V_S}{\kappa T_E}\right)^{1/2}\right]\exp\left(\frac{e\,\Delta V_S}{\kappa T_E}\right)}{\left(\frac{2\kappa T_E}{\pi m_e}\right)^{1/2}} + \frac{j_{e,P}\operatorname{erf}\left(\frac{e\,\Delta V_S}{\kappa T_{e,P}}\right)^{1/2}}{\left(\frac{2\kappa T_{e,P}}{\pi m_e}\right)^{1/2}} - \frac{j_{i,E}\exp\left(-\frac{e\,\Delta V_S}{\kappa T_E}\right)}{\left(\frac{2\kappa T_E}{\pi m_i}\right)^{1/2}} \tag{27}$$

The fact that the last term equals half of the ion charge density in the plasma permits a reasonably direct estimate of the overall sheath drop ΔV_S.

Electron sheath (electron potentials are negative numbers.) -

$$\rho_{\Delta V} = \frac{j_{e,E}\left[1 + \operatorname{erf}\left(-\frac{e\,\Delta V}{\kappa T_E}\right)^{1/2}\right]\exp\left[\frac{e(\Delta V_S - \Delta V)}{\kappa T_E}\right]}{\left(\frac{2\kappa T_E}{\pi m_e}\right)^{1/2}}$$

$$+ \frac{j_{e,P}\left[1 - \operatorname{erf}\left(-\frac{e\,\Delta V}{\kappa T_{e,P}}\right)^{1/2}\right]\exp\left(-\frac{e\,\Delta V}{\kappa T_{e,P}}\right)}{\left(\frac{2\kappa T_{e,P}}{\pi m_e}\right)^{1/2}}$$

$$- \frac{j_{i,E}\left\{1 - \operatorname{erf}\left[-\frac{e(\Delta V_S - \Delta V)}{\kappa T_E}\right]^{1/2}\right\}\exp\left[-\frac{e(\Delta V_S - \Delta V)}{\kappa T_E}\right]}{\left(\frac{2\kappa T_E}{\pi m_i}\right)^{1/2}}$$

$$- \frac{j_{i,P}\left\{1 + \operatorname{erf}\left[-\frac{e(\Delta V_S - \Delta V)}{\kappa T_{i,P}}\right]^{1/2}\right\}\exp\left(\frac{e\,\Delta V}{\kappa T_{i,P}}\right)}{\left(\frac{2\kappa T_{i,P}}{\pi m_i}\right)^{1/2}} \tag{28}$$

For $\Delta V = 0$,

$$\rho_P = 0 = \frac{j_{e,E} \exp\left(\frac{e\,\Delta V_S}{\kappa T_E}\right)}{\left(\frac{2\kappa T_E}{\pi m_e}\right)^{1/2}} - \frac{j_{i,E}\left[1 - \operatorname{erf}\left(-\frac{e\,\Delta V_S}{\kappa T_E}\right)^{1/2}\right]\exp\left(-\frac{e\,\Delta V_S}{\kappa T_E}\right)}{\left(\frac{2\kappa T_E}{\pi m_i}\right)^{1/2}} - \frac{j_{i,P} \operatorname{erf}\left(-\frac{e\,\Delta V_S}{\kappa T_{i,P}}\right)}{\left(\frac{2\kappa T_{i,P}}{\pi m_i}\right)^{1/2}} \tag{29}$$

Here, the first term equals half of the electron charge density in the plasma and allows a simple estimate of ΔV_S.

Sheath Configurations

Expressions for charge densities and Poisson's equation lead to sheath fields and potentials as functions of distance.

Electric fields:

$$\frac{d}{dx}\left(\frac{dV}{dx}\right)^2 = 2\,\frac{dV}{dx}\,\frac{d^2V}{dx^2} = -8\pi\rho\,\frac{dV}{dx}$$

$$E_{\Delta V} = -\frac{dV}{dx} = \pm\left(-8\pi \int_0^{\pm\Delta V} \rho_{\Delta V}\, dV\right)^{1/2} \tag{30}$$

Distances:

$$x = 0 \quad \text{at} \quad \Delta V = \Delta V_S$$

$$x = x_P \quad \text{at} \quad \Delta V = 0$$

$$x_P - x = -\int_{\Delta V}^{0} \frac{dV}{E}$$

$$x_{\Delta V} = -\int_{\Delta V_S}^{0} \frac{dV}{E} + \int_{\Delta V}^{0} \frac{dV}{E} = \int_{\Delta V}^{\Delta V_S} \frac{dV}{E} \tag{31}$$

The program evaluates these integrals as sums of trapezoids based on 20 equal increments of ΔV from zero to ΔV_S. Equation (30) causes no problem, and as far as the machine is concerned, neither does equation (31). But when $\Delta V = 0$, $E = 0$, and equation (31) is undefined. The machine, however, merely takes half of the value of E for $\Delta V_S/20$. That average E used for the first ΔV increment produces a finite x_P. This distance is an effective sheath width, which includes much of the sheath structure. The applicability of this definition derives from the extent to which it represents a fully developed sheath. If the charges nearly balance at x_P, the effective sheath width offers utility - particularly when x_P is a few Debye lengths rather than an incessant infinity (refs. 31 to 34).

Locations for these plasma, sheath interfaces result from a simple process: First, select the retarded flow from the emitter (ions for ion sheaths and electrons for electron sheaths). Next, set the number density of this flow at the effective sheath, plasma interface equal to half of the number density of the plasma electrons. Then, compute the sheath potential drop (eqs. (27) and (29)). Finally, use the overall voltage change in the field and distance integrals to determine an effective sheath thickness.

Justification of this concept appears in DISCUSSION OF RESULTS.

Calculation Method

Before the main calculations a simple screening obviates many permutations of conditions precluded by the model: First, the electrode temperature must be low enough to maintain an effective solid emitter. Next, the cesium pressure in the plasma must be below its vapor pressure (ref. 30) at the emitter temperature to prevent continuous condensation of cesium. And, finally, the Debye length must be shorter than the mean free path for cesium charge exchange (ref. 29) to make the sheath essentially collisionless. The last condition was selected because the distances between cesium charge exchanges are less than the lengths between elastic encounters of electrons and neutrals, the resonance exchanges of free and bound electrons, and the coulombic collisions at the resulting plasma conditions. The model admits no collective interactions and allows only collisions beginning and ending with singly ionized and ground-state atoms and electrons.

If a set of parameters passes this screening, that system enters the primary computing process. The iterative sheath solution follows an almost classic numeric recipe:

(1) Solve for current densities deleting effects of sheath fields (eqs. (4) and (5) with (7), (8), and (27) or (18), (19), and (29)).

(2) From the first step also obtain an estimate of the potential drop across the sheath (eq. (27) or (29)).

(3) Divide the overall voltage change into 20 increments and compute charge densities for increasing potentials through the sheath (eq. (26) or (28)).

(4) Integrate numerically the charge density function (from the third step) over the voltage to yield the sheath field (eq. (30)).

(5) Use the field at the virtual Schottky emitter and the potential fall across the sheath to produce new current densities for emissions (first step).

(6) Repeat the cycle until no boundary current density that the sheath affects (eqs. (10), (11), (21), and (22)) changes by more than 0.1 percent of the smallest boundary current density.

(7) Integrate numerically the negative reciprocal of the electric field over voltage to determine sheath distances (eq. (31)).

DISCUSSION OF RESULTS

For all of the temperatures (1000° to 3000° K) and plasma densities (10^{12} to 10^{16} cm^{-3}), equilibria between emitters and ionized gases occur at work functions dictated by the Saha-Langmuir theory. As figure 1 indicates, the null-point work functions vary directly with minus the logarithm of electron number density and almost directly with temperature.

These null-point work functions also serve as plasma potentials ($\Delta V = 0$) relative to emitter Fermi levels for all systems analyzed here except the positive-ion sheaths with the plasma electron temperature elevated above that of the emitter, ions, and atoms. For these nonequilibrium positive-ion sheaths, figure 1 shows that plasma potentials branch away from the Saha-Langmuir curves. The offshoots represent the variation of electron potentials with electron temperature when atom, ion, and emitter temperatures are fixed at the value for no elevation of plasma electron temperature ($\Delta T_{e,P} = 0$). Only the potential and temperature of the plasma electrons change along any one of the branch curves.

For these nonequilibrium ion sheaths, potentials of the plasma electrons, with given values of temperature elevation and number density lie above the Saha-Langmuir value at lower temperatures and below it at higher temperatures. This trend results from changes in ion emission, which strongly influences the formation of the positive-ion sheath. The changes involve two contesting effects: If the temperature for the ions, atoms, and emitter drops below the temperature of the electrons, random currents sup-

plying cesium from the plasma to the emitter decrease, and the fraction of cesium leaving the emitter as ions increases.

At the reduced ion and atom temperature and a given charge number density, the plasma atom concentration is identical with that for the same system with all temperatures at the electron value. Being proportional to the square root of the temperature, though, the average random cesium velocity in any direction is less. Cesium ions and atoms move more slowly toward the emitter, lowering ion emission proportionately. This reduction is relatively large for a specified elevation of electron temperature at low temperatures. Thus, the plasma electron potential for the nonequilibrium positive-ion sheath rises above the Saha-Langmuir value as the general temperature level falls.

This influence decreases as the general temperature level rises; then the second mechanism gains control. Decreasing the emitter temperature increases the fractional ion emission (eqs. (3) and (8)), often almost exponentially for the nonequilibrium positive-ion sheath. At high temperatures, therefore, reducing ion, atom, and emitter temperatures together yields a net gain in ion production. And the plasma electron potential drops below the isothermal value.

Although elevating plasma electron temperatures affects plasma potentials for the nonequilibrium ion sheath, it fails to change plasma potentials for the nonequilibrium electron sheath. This effect results from the major influence of emitted electrons on the structure of the electron sheath. The barrier reflects the high number densities of low-energy emitted electrons back to the emitter; only an exponentially cutoff flow escapes. But this small exodic current nearly balances the injection of electrons into the sheath from the plasma. Plasma electrons, therefore, affect these electron sheaths insignificantly. And the rate of escape of electrons from the emitter remains the same - unaltered by plasma and sheath conditions. Thus, elevation of the plasma electron temperature causes practically no change in the electron sheath at an emitter.

For equilibria the criteria for collisionless ion and electron sheaths were satisfied with 10^{12}, 10^{13}, and 10^{14} electrons per cubic centimeter at 2400° K and with 10^{12} and 10^{13} at 2000° K. Figure 3 describes these systems, which include work functions from 1.5 to 5.0 volts, Debye lengths from 3.4×10^{-5} to 3.4×10^{-4} centimeter, and plasma potentials from 3.0 to 4.2 volts. The parameters appear in the insert. In figure 3 the dependent and independent variables are dimensionless. The ordinates are the effective sheath width (x_S/λ_D), sheath drop ($\Delta V_S/\Delta V_o = \Delta V_S/(\varphi - \varphi_o)$), and emitter field ($E_E\lambda_D/(\varphi - \varphi_o)$). All abscissae are Richardson-Dushman (R-D) drops ($|e\,\Delta V_o|/\kappa T = e|\varphi - \varphi_o|/\kappa T$).

Similar results for some nonequilibrium ion and electron sheaths appear in figure 4. The elevations of electron temperatures account for the increased ranges of parameters that satisfy the collisionless criteria (1600°, 2000°, and 2400° K and 10^{12}, 10^{13}, 10^{14}, 10^{15} electrons/cm^3).

The present method yields effective sheath widths for the retarded particles from the emitter (for electrons in an electron sheath or for ions in an ion sheath). In contrast with those for equilibria (fig. 3), the effective sheath widths in figure 4 scatter more widely about their mean. But the trends and levels of results are comparable for equilibrium and nonequilibrium ion and electron sheaths.

This paper defines a sheath system as near-equilibrium when the net current of each kind of particle falls below 6 percent of its corresponding random plasma current. Figure 5 shows the portion of the data of figure 4 that satisfy this criterion. The same set of curves correlates both electrons and ion sheaths, although the expanded sheath-width scale accentuates separations.

The correlations of figures 4 and 5 exemplify traditional treatments of sheath characteristics - in terms of number density, temperature, and Debye lengths for plasma electrons. For these Saha plasmas contiguous with Saha-Langmuir emitters, however, emission dominates the sheaths (eqs. (13) and (14)). Where the ionized gas meets the electrode, the energy of the emitted particles influences charge separation to a greater extent than the plasma-electron temperature. The sheath data, therefore, should organize more readily around functions of plasma-electron number density and emitter temperature. One such function is the emission Debye length $\lambda_{DE} \approx 6.9(T_E/N_{e,P})^{1/2}$

Figure 6 shows the nonequilibrium sheath data correlated with emitter temperature rather than plasma-electron temperature. Results for both ion and electron sheaths compact around the dashed curves for equilibria above R-D drops of $2\frac{1}{2}$ to 3. Below this region, though, reducing overall voltages moves nonequilibrium sheaths away from equilibria and renders these calculations inapplicable.

The good correlations in figure 6 indicate that sheath characteristics depend strongly on emitter temperature, plasma-electron number density, and emission Debye length when emitted particles control transitions between plasmas and electrodes.

Figure 7 shows trends of the ratio of the minority-charge density at the effective sheath width to that in the neutral plasma as functions of R-D drop. These calculations indicate that the charge imbalance decreases below 1 percent of the number density of plasma electrons when the R-D drop increases above $2\frac{1}{2}$ to $3\frac{1}{2}$. For equilibrium and near-equilibrium systems, then, the effective sheath width seems a meaningful concept.

The number density of the majority charge at the emitter appears as a function of R-D drop in figure 8, which includes all equilibrium and nonequilibrium data for ion and electron sheaths. The rise in majority charge and consequently gas density near the emitter results from retarded and reflected emission. Approaching the emitter through the sheath, the density of the minority charge falls below that in the plasma. The atom density remains unchanged. But the density of the dominant charge climbs to a maximum at the emitter even though the contribution to that density by flow from the plasma decreases because of acceleration.

Figure 8 reveals that the majority-charge density at the emitter depends only on plasma charge number density and the R-D drop containing the emitter temperature. This simple plot further supports the concept of the emission Debye length ($\lambda_{DE} \approx 6.9(T_E/N_{e,P})^{1/2}$) as a correlation parameter.

The trends in figure 8 indicate that the charge number density can gain two orders of magnitude while moving from the plasma to the emitter through a 1-volt sheath. Of course, at Saha-Langmuir null points, with no sheaths, the gas density remains constant throughout.

The present results reinforce many past findings that properties based on bulk-gas distributions are not meaningful within a few mean free paths of a confining wall (refs. 35 to 38). This generalization usually holds even when gradients are small at the boundary. Consider a simple thermally randomized gas in a container: Unless the wall injects the same kinds of particles in the same proportions at the same rates with the same energy distributions as those it receives from the gas, the distribution changes abruptly within several collision lengths from the wall. If the gas moves relative to the container, the problem is further complicated. A solid surface cannot supply random distributions displaced around drift velocities unless it moves at those velocities. In the absolute sense, then, even the mean free path, computed using the bulk-gas distribution, means nothing at the usual confining boundary.

The exception occurs when the boundary returns particle flows that maintain the distributions in the bulk-gas. In a plasma this ideal mating of a solid surface and a thermally randomized gas happens at the Saha-Langmuir null point. When emissions of electrons, ions, and atoms fail to balance their random plasma currents, however, sheaths generally grow. And as figure 8 implies, distributions can change rapidly even in static isothermal systems.

In this study, though, the screening calculations used the distributions of the plasmas to estimate collisions in the sheaths. On this basis cesium charge exchange dominates particle encounters over the ranges of plasma conditions used. To be more correct, the coulombic tests should have utilized mean free paths averaged over the charge-distribution changes of the sheaths. But this test requires the prior complete solution of the sheath. The additional complication was deemed unwarranted for these approximations.

All of the previous discussion dealt with sheath structure. In addition to connecting the plasma and surface potentials, though, the sheath influences charge flow. To illustrate some transport effects, figure 9 gives net current densities as functions of R-D drops for all nonequilibrium sheaths in this study ($T_{e,P} > T_E = T_{i,P} = T_{a,P}$). Because the elevated temperatures of plasma electrons unbalance these systems, the net electron currents flow to the electrodes as figure 9 indicates. For this reason electron temperature rather than emitter temperature might serve better in the R-D drop. The

change tightens the correlation a bit but not enough to justify the inconsistency of representation.

The curves for current densities through electron sheaths extend horizontally down to R-D drops near 1; below that they fall off slightly. These practically constant currents almost equal the increases of plasma-electron random currents caused by the higher plasma electron temperatures. When the higher electron currents from the plasmas enter the sheaths built primarily by electron emission, they accelerate toward the emitter, which completely absorbs them.

Electron sheaths with small overall potential drops, where electron currents from the emitters and plasmas are similar, react to plasma changes. At low R-D drops the net negative current through the electron sheaths from the plasma falls off because of rise in the net ion current to the emitter. If only plasma electron temperatures increase at constant charge number densities, random currents of atoms diminish in these ionized gases (eq. (1)). The decreased supplies of atoms reduce ion emissions and allow higher net ion currents toward the emitters.

Figures 5 and 6 indicate that near-equilibrium exists for R-D drops greater than $2\frac{1}{2}$ to 3. For these R-D values, the applicable current densities of figure 9 run from less than 10^{-4} to more than 10^{2} amperes per square centimeter.

To this point, only overall results received attention. Now figures 10 to 13 present detailed structures for some ion and electron sheaths separating emitters at 2000° K from plasmas with 10^{13} electrons per cubic centimeter. In the ionized gas, ion and atom temperatures are also 2000° K while electron temperatures are either 2000° or 2200° K. For each of the four sets of conditions, four work functions cause sheath drops to range from 0 to over 0.95 volt. Tables give incremental potential changes, charge densities, electric fields, and distances. Tabulations of overall sheath characteristics also appear. Finally, plots compare Richardson-Dushman and Schottky results to indicate significant errors caused by omitting effects of fields on emissions. Appendix B defines the symbols for the IBM output sheets.

As expected, figures 10 to 13 show that absolute rates of change of electric fields and potentials, as functions of sheath distance, maximize at the emitter and minimize at the plasma. Curves for majority-charge densities bow strongly toward the origins. But curves for minority-charge densities bulge away from the origins for overall sheath drops near 0 volt and toward the origins for overall sheath drops near 1 volt. Apparently simple models like exponential variations of both charges with dimensionless voltages fail to describe this kind of sheath.

CONCLUDING REMARKS

In these sheaths, which separate Saha plasmas from Schottky Saha-Langmuir emitters, emissions control charge densities. For ion sheaths raising only the electron temperature in the plasma with a given charge number density reduces the sheath drops. This reduction results from decreasing the supply of atoms to the emitter and thus diminishing ion emission. For sizeable electron sheaths, however, raising the plasma electron temperatures has a negligible effect because the electron emission remains unchanged. Since the emitter dominates the sheaths, the emission Debye length $6.9(T_E/N_{e,P})^{1/2}$ correlates their characteristics better than the usual plasma Debye length $6.9(T_{e,P}/N_{e,P})^{1/2}$.

Effective widths for equilibrium and near-equilibrium sheaths in the present study lie between 2 and 2.6 emission Debye lengths. Corresponding values of work function minus plasma potential both divided by the voltage equivalent of emitter temperature range from near 0 to 10. As this dimensionless voltage variable closely approaches 0, the effective sheath width and the overall sheath voltage differences drop toward 0. For values of the dimensionless voltage variable greater than 2, the sheath drops stabilize between 0.8 and 1.0 times the work function minus the plasma potential.

These generalizations apply to equilibrium and near-equilibrium results. In the present work, near-equilibria occur at values of the dimensionless voltage variable above $2\frac{1}{2}$ to 3. This lower limit begins the region where net particle current densities through the sheaths are less than 6 percent of their random circulations in the plasmas. Also for voltage variables above $2\frac{1}{2}$ to 3, charge imbalances at effective sheath widths are below 1 percent of plasma electron number densities.

Accumulations of cesium in positive-ion sheaths at high work-function surfaces complicate these systems. When emitters adsorb cesium, work functions generally decrease; cesium arrivals from the plasma alone lower the work function of the bare emitter. But with positive-ion sheaths, the greater ion concentration near the electrode increases cesium transport and changes the work function even more. Although these phenomena caused no problems in the present parametric study, in practice the work function depends on the emitter, the plasma, and the sheath.

The near-equilibrium sheaths of this study pass net electron currents to the electrodes rather than to the plasma. Some of the current densities exceed 100 amperes per square centimeter. At present, though, net electron flows from the emitter to the plasma hold more interest, particularly in thermionic energy conversion. Applying an appropriate field lowers the sheath potential and allows electron emission to overrun the excess currents caused by elevated plasma electron temperatures. Then the problems of accelerated charge distributions in the plasmas grow. Streams of excess electrons falling through sizeable potential drops enhance local ionization and often start collec-

tive oscillations (ref. 39). Such complications far exceed those of the present calculations.

But this sheath model allows net electron flows from, as well as to, the electrodes. At the conditions analyzed here, for example, lowered rather than elevated plasma electron temperatures produce electronic emitters rather than collectors.

The model fits some heterothermal systems particularly well: For retarded plasma particles, an increased rise in sheath potential results in smaller current exchanges with the electrode; then the model tolerates larger temperature differences between the opposing streams. The atoms and accelerated particles from the ionized gas undergo essentially complete replacements at the plasma, sheath interface by flows from the emitter. Thus, the model requires nearly isothermal trades of these species. Such precautions aim at preserving the specified state of the plasma. Restrictions to small net transport densities relative to random plasma circulations assure minor perturbations.

Within its limitations, this sheath method analyzes equilibria, estimates near-equilibria, and gives some insight into certain systems capable of high power outputs. But the near-equilibrium criterion limits the current densities and temperature differences of potentially high-power systems in analyses of this kind.

Lewis Research Center,
National Aeronautics and Space Administration,
Cleveland, Ohio, July 20, 1967,
120-33-02-01-22.

APPENDIX A

SYMBOLS

E	electric field
e	electronic unit charge
h	Planck's constant
I	ionization potential
J	overall net current density
j	particle current density or net particle current density
m	particle mass
N	particle number density
p	pressure
T	absolute temperature
V	potential
ΔV	potential relative to plasma potential
x	distance from emitter
κ	Boltzmann constant
λ	mean free path for cesium charge exchange in emitter temperature range
λ_D	plasma Debye length, $\approx 6.9(T_{e,P}/N_{e,P})^{1/2}$, cm
λ_{DE}	emission Debye length, $\approx 6.9(T_E/N_{e,P})^{1/2}$, cm
ρ	charge density
φ	work function
φ'	effective work function for virtual Schottky emitter
φ_o	work function (plasma potential) that precludes an ion sheath
φ_{oo}	work function (plasma potential) that precludes an electron sheath

Subscripts:

a	atom
E	emitter
e	electron
i	ion
o	to work function (from plasma potential)
P	plasma
S	overall sheath
vp	vapor pressure
ΔV	at ΔV

APPENDIX B

NOMENCLATURE FOR IBM OUTPUT

FORTRAN symbol	Algebraic symbol	Description	Units
I	I	ionization potential for plasma atoms	V
TE	T_E	emitter temperature	^oK
PHI	φ	work function	V
NEP	$N_{e,P} = N_{i,P}$	plasma electron number density	cm^{-3}
TEP	$T_{e,P}$	plasma electron temperature	^oK
TIP	$T_{i,P} = T_{a,P}$ for these solutions	plasma ion temperature	^oK
LAMBDA	$\lambda_D \approx 6.9(T_{e,P}/N_{e,P})^{1/2}$	plasma Debye length	cm
PV	P_{vp}	vapor pressure of plasma element at T_E	torr $(N/m^2/133.322)$
LAMBDA(TE)	$\lambda_{DE} \approx 6.9(T_E/N_{e,P})^{1/2}$	emission Debye length	cm
DV	ΔV	sheath potential measured from plasma electron potential	V
ND(DV)	$N_{e,\Delta V} - N_{i,\Delta V}$	net number density of charge at ΔV	cm^{-3}
NE(DV)	$N_{e,\Delta V}$	electron number density at ΔV	cm^{-3}
NI(DV)	$N_{i,\Delta V}$	ion number density at ΔV	cm^{-3}
E(DV)	$E_{\Delta V}$	electron electrostatic field at ΔV	V/cm
X(DV)	$x_{\Delta V}$	distance from emitter to ΔV	cm
JEE	$j_{e,E}$	emitted electron current density	A/cm^2
JEP	$j_{e,P}$	plasma electron random current density	A/cm^2
JIP	$j_{i,P}$	plasma ion random current density	A/cm^2

FORTRAN symbol	Algebraic symbol	Description	Units
JAP	$j_{a,P}$	plasma atom equivalent random current density	A/cm^2
J	J	net current density through sheath	A/cm^2
PP	p_p	plasma pressure	torr ($N/m^2/133.322$)
JIE	$j_{i,E}$	emitted ion current density	A/cm^2
JAE	$j_{a,P}$	emitted equivalent atom current density	A/cm^2
JA	j_a	net equivalent atom current density	A/cm^2
JI	j_i	net ion current density	A/cm^2
JE	j_e	net electron current density	A/cm^2
JA/JAP	$j_a/j_{a,P}$	----------	------
JE/JEP	$j_e/j_{e,P}$	----------	------
JI/JIP	$j/j_{i,P}$	----------	------
DVS	ΔV_S	overall sheath voltage drop	V
XDVS	$x_{\Delta V_S} = x_P = x_S$	effective sheath thickness	cm
NAP	$N_{a,P}$	plasma atom number density	cm^{-3}
XDLAM	X_S/λ_D	----------	------
SC	$(e^3 E_E)^{1/2}$	Schottky depression of work function	V
PHZ	φ_o	plasma potential (work function for no sheath)	V
EDVS	$E_{\Delta V_S} = E_E$	electrostatic field at the emitter	V/cm
DVSRD	$\Delta V_0 = \varphi - \varphi_o$	Richardson-Dushman overall sheath voltage drop	V
DVS/RD	$\Delta V_S/\Delta V_0 = \Delta V_S/(\varphi - \varphi_o)$	----------	------
ELM/RD	$E_E \lambda_D/(\varphi - \varphi_o)$	----------	------

FORTRAN symbol	Algebraic symbol	Description	Units
PHZZ	$\varphi_{oo} = \varphi_o$ for equilibrium and electron sheaths	plasma potential at equilibrium (work function for no sheath and no net current)	V
DRD/KT	$e\lvert\varphi - \varphi_o\rvert/\kappa T_e$	----------	------
NTP	----------	total particle number density in plasma	cm^{-3}
NCE	----------	total charge number density at emitter	cm^{-3}
NTE	----------	total particle number density at emitter	cm^{-3}
RD/KTE	$e\lvert\varphi - \varphi_o\rvert/T_E$	----------	------
X/LMTE	x_S/λ_{DE}	----------	------
ELT/RD	$E_E\lambda_{DE}/(\varphi - \varphi_o)$	----------	------
NEPA	----------	plasma electron number density from sheath calculations	cm^{-3}

REFERENCES

1. Langmuir, Irving; and Kingdon, K. H.: Contact Potential Measurements with Absorbed Films. Phys. Rev., vol. 34, no. 1, July 1, 1929, pp. 129-135.

2. Richardson, O. W.: Negative Radiation From Hot Platinum. Cambridge Phil. Soc. Proc., vol. 11, Feb. 1902, pp. 286-295.

3. Dushman, S.: Electron Emission from Metals as a Function of Temperature. Phys. Rev., vol. 21, June 1923, pp. 623-636.

4. Dushman, Saul: Thermionic Emission. Rev. Mod. Phys., vol. 2, no. 4, Oct. 1930, pp. 381-476.

5. Saha, M. N.: Ionization in the Solar Chromosphere. Phil. Mag., vol. 40, Oct. 1920, pp. 472-488.

6. Kaminsky, Manfred: Atomic and Ionic Impact Phenomena on Metal Surfaces. Academic Press, 1965.

7. Cobine, James D.: Gaseous Conductors Theory and Engineering Applications. Dover Publications, 1941.

8. Wilkins, Daniel R.; and Gyftopoulos, Elias P.: Thermionic Converters Operating in the Ignited Mode. Part II: A Quasi-Equilibrium Model for the Interelectrode Plasma. J. Appl. Phys., vol. 37, no. 7, June 1966, pp. 2892-2899.

9. Nottingham, Wayne B.; and Breitwieser, Roland: Theoretical Background for Thermionic Conversion Including Space-Charge Theory, Schottky Theory, and the Isothermal Diode Sheath Theory. NASA TN D-3324, 1966.

10. Mott-Smith, H. M.; and Langmuir, Irving: The Theory of Collectors in Gaseous Discharges. Phys. Rev., vol. 28, no. 4, Oct. 1926, pp. 727-763.

11. Bohm, D.: Minimum Ionic Kinetic Energy for a Stable Sheath. The Characteristics of Electrical Discharges in Magnetic Fields. A. Guthrie and R. K. Wakerling, eds., McGraw-Hill Book Co., Inc., 1949, pp. 77-86.

12. Boyd, R. L. F.: The Collection of Positive Ions by a Probe in an Electrical Discharge. Roy. Soc. Proc., ser. A., vol. 201, no. 1066, Apr. 26, 1950, pp. 329-347.

13. Schulz, George J.; and Brown, Sanborn C.: Microwave Study of Positive Ion Collection by Probes. Phys. Rev., vol. 98, no. 6, June 15, 1955, pp. 1642-1649.

14. Loeb, Leonard B.: Basic Processes in Gaseous Electronics. Second ed., Univ. California Press, 1955.

15. Auer, Peter L.: Potential Distributions in a Low-Pressure Thermionic Converter. J. Appl. Phys., vol. 31, no. 12, Dec. 1960, pp. 2096-2103.

16. Nottingham, Wayne B.: Sheath and Plasma Theory of an Isothermal Diode. Rep. No. 4-62, Thermo Electron Eng. Corp., Oct. 1962.

17. Caruso, A.; and Cavaliere, A.: The Structure of the Collisionless Plasma-Sheath Transition. Nuovo Cimento, vol. 26, no. 6, Dec. 16, 1962, pp. 1389-1404.

18. Chen, F. F.: Probe Techniques. Plasma Physics Summer Institute, Lecture Notes, Princeton University, 1962.

19. Chen, F. F.: Numerical Computations for Ion Probe Characteristics in a Collisionless Plasma. J. Nucl. Energy, Part C - Plasma Phys., vol. 7, no. 1, 1965, pp. 47-67.

20. Gurevich, A. V.: Structure of the Disturbed Zone in the Neighborhood of a Large Charged Body in Plasma. Geomagnetism and Aeronomy, vol. 3, no. 6, 1963, pp. 822-832.

21. Self, S. A.: Exact Solution of the Collisionless Plasma-Sheath Equation. Phys. Fluids, vol. 6, no. 12, Dec. 1963, pp. 1762-1768.

22. Cohen, Ira M.: Asymptotic Theory of Spherical Electrostatic Probes in a Slightly Ionized, Collision-Dominated Gas. Phys. Fluids, vol. 6, no. 10, Oct. 1963, pp. 1492-1499.

23. Lyubimov, G. A.: Electrical Potential Variation Layers Near Electrodes. Proceedings of the International Symposium on Magnetohydrodynamic Electric Power Generation, European Nuclear Energy Agency, Paris, July 6-11, 1964, paper 7a, pp. 125-130.

24. Lam, S. H.: Unified Theory for Langmuir Probe in Collisionless Plasma. Phys. Fluids, vol. 8, no. 1, Jan. 1965, pp. 73-87.

25. Heyman, R. J.; and Fenster, S. J.: Electrical Surface Interaction in Hypersonic Flight. I: The Aerodynamic Plasma Sheath. J. Astron. Sci., vol. 12, no. 2, Summer 1965, pp. 51-58.

26. Wasserstrom, E.; Su, C. H.; and Probstein, R. F.: Kinetic Theory Approach to Electrostatic Probes. Phys. Fluids, vol. 8, no. 1, Jan. 1965, pp. 56-72.

27. LeBihan, R.; and Maugis, D.: Etude Theoretique et Experimentale de Structures Creuses a Plasma de Cesium, Sources D'Ions ou D'Electrons. Ann. Radioelectricite, vol. 20, Apr. 1965, pp. 126-158.

28. Schottky, Walter: Über den Austritt von Elektronen aus Glühderähten bei Verzögernden Potentialen. Ann. Physik, vol. 44, 1914, pp. 1011-1032.

29. Sheldon, John W.: Mobilities of the Alkali Metal Ions in Their Own Vapor. J. Appl. Phys., vol. 34, no. 2, Feb. 1963, p. 444.

30. Heimel, Sheldon: Thermodynamic Properties of Cesium up to 1500° K. NASA TN D-2906, 1965.

31. Okuda, T.; and Yamamoto, K.: A New Probe Method for Measuring Ionized Gases. Phys. Soc. Japan J., vol. 13, no. 4, Apr. 1958, pp. 411-418.

32. Bettinger, Richard T.; and Walker, Evan H.: Relationship for Plasma Sheath About Langmuir Probes. Phys. Fluids, vol. 8, no. 4, Apr. 1965, pp. 748-751.

33. Nation, J. A.; and Simpson, D.: Probes in Atmospheric Pressure Argon Plasma. Brit. J. Appl. Phys., vol. 16, no. 11, Nov. 1965, pp. 1699-1704.

34. Nation, J. A.; and Simpson, D.: A Measurement of the Effective Thickness of the Plasma Sheath at a Cold Electrode. Brit. J. Appl. Phys., vol. 16, no. 11, Nov. 1965, pp. 1705-1709.

35. Mott-Smith, Harold M.: A New Approach in the Kinetic Theory of Gases. Group Rep. V-2, Lincoln Lab., Mass. Inst. Tech., Dec. 1954.

36. Wang Chang, C. S.; and Uhlenbeck, G. E.: On the Behavior of a Gas Near a Wall; a Problem of Kramers'. Rep. No. 2457-2-T, Eng. Res. Inst., Univ. Michigan, Aug. 1956. (Available from DDC as AD-111875).

37. Gross, E. P.; Jackson, E. A.; and Zearing, S.: Boundary-Value Problems in the Kinetic Theory of Gases. Rep. No. AFOSR TN-56-527, Office of Scientific Research, 1956. (Available from DDC as AD-11036).

38. Morris, J. F.: Physico-Chemical Reactions During Nozzle Flow. The Chemistry of Propellants. S. S. Penner and J. DuCarme, eds., Pergamon Press, 1960, pp. 410-490.

39. Moreau, J. B.: Oscillations et Distribution Non Maxwellienne des Electrons dans un Plasma de Cesium. J. Physique, vol. 26, Aug.-Sept. 1965, pp. 448-450.

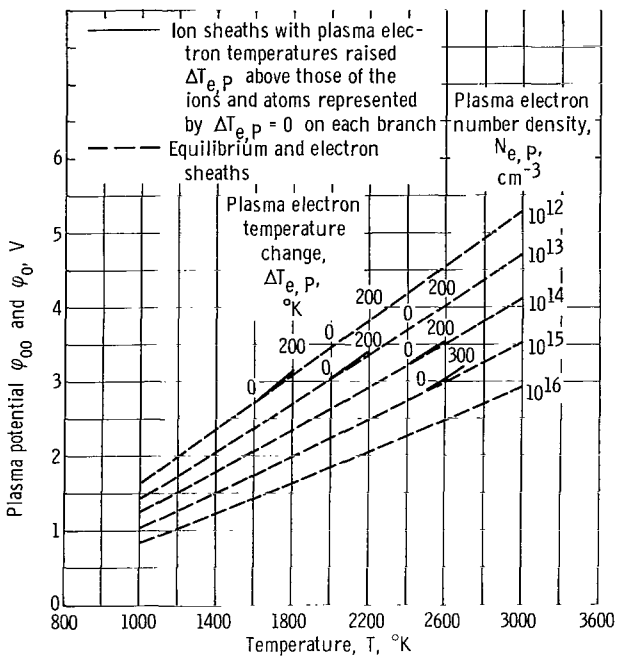

Figure 1. - Work functions that preclude sheaths between emitters and cesium Saha plasmas (plasma potentials).

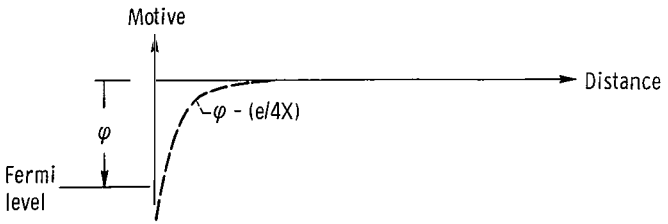

(a) Emission motive for electrons and singly charged positive ions.

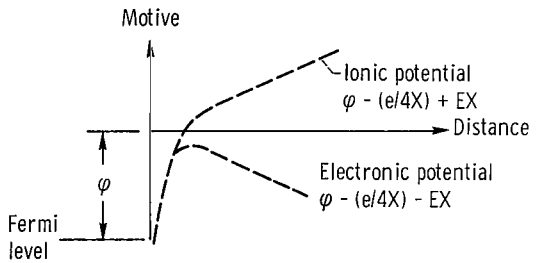

(b) Emission motives in constant external electrostatic field.

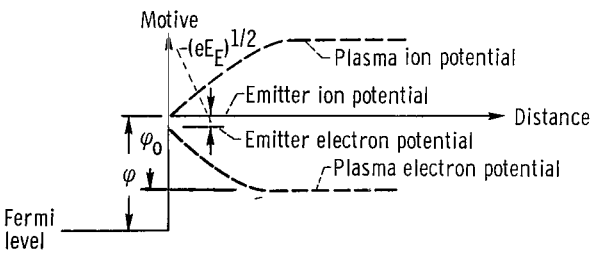

(c) Traditional thermionic emitter with positive-ion sheath.

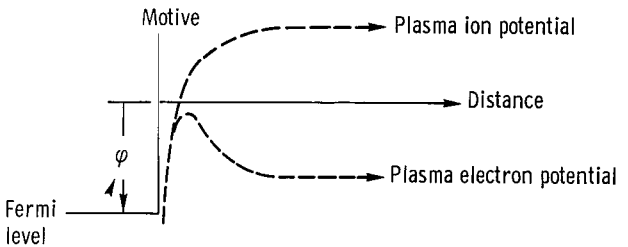

(d) Superposed image and sheath potentials.

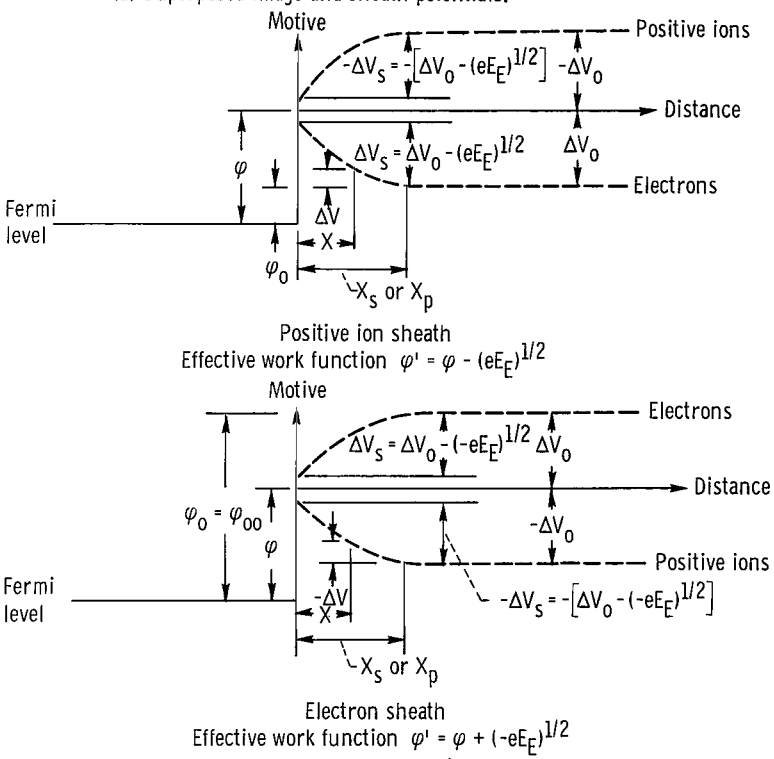

(e) Virtual Schottky emitters.

Figure 2. - Development of virtual Schottky emitters.

Overall sheath voltage drop / (Work function) - (Plasma potential)
$\frac{\Delta V_s}{\psi - \psi_\infty}$
1.0
.9
.8
.7
Sheath width / Debye length
$\frac{\chi_s}{\lambda_D}$
2.8
2.6
2.4
2.2
2.0

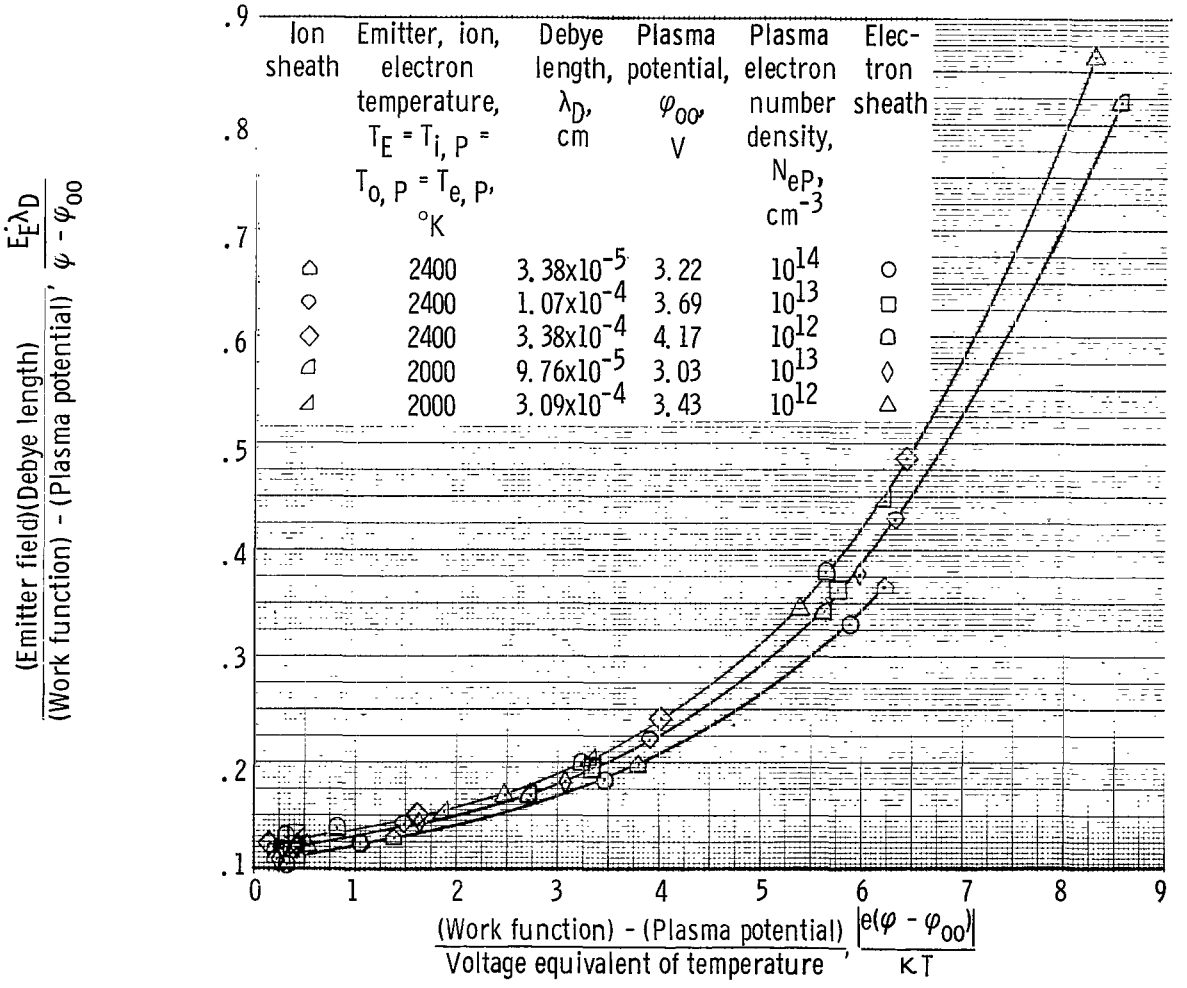

Figure 3 - Equilibrium (isothermal) collisionless ion ($\varphi > \varphi_{00}$) and electron ($\varphi < \varphi_{00}$) sheaths.

Overall sheath voltage drop / (Work function) - (Plasma potential)
$\frac{\Delta V_s}{\varphi - \varphi_o}$
Sheath width / Debye length, $\frac{X_s}{\lambda_D}$
1.0
.8
.6
.4
2.5
2.1
1.7
1.3
.9
.5
1
2
3
5, 7
10
4
6
9
13
11
8
12
6, 7
10, 11
12, 13
8, 9
2, 3
4, 5

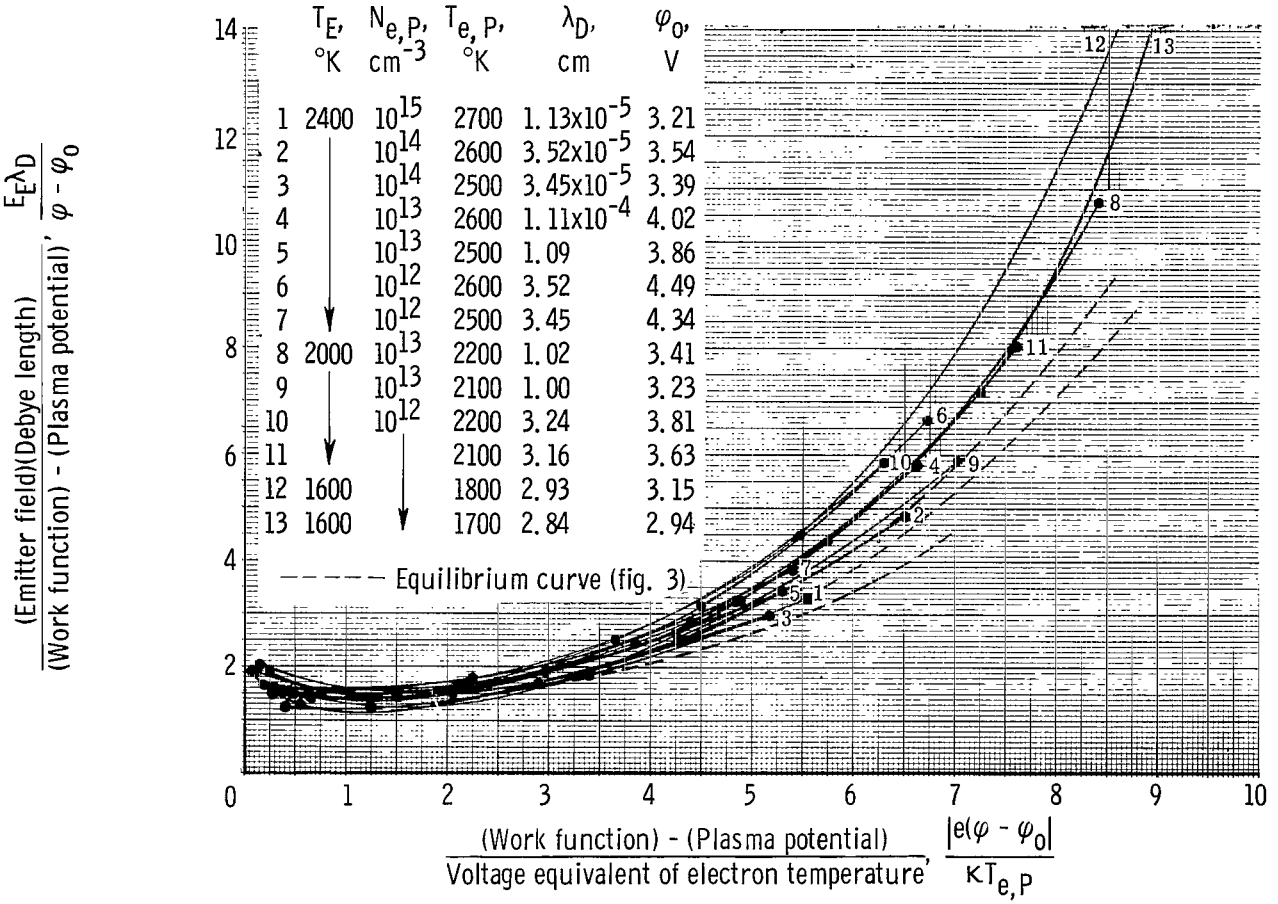

(a) Ion ($\varphi < \varphi_0$) sheaths.

Figure 4. - Nonequilibrium ($T_{e,P} > T_E = T_{i,P} = T_{a,P}$) collisionless sheaths.

Overall sheath voltage drop / (Work function) - (Plasma potential), $\frac{\Delta V_s}{\varphi - \varphi_{oo}}$
Sheath width / Debye length, $\frac{\chi_s}{\lambda_D}$
1.0
.8
.6
.4
.2
2.7
2.3
1.9
1.5
1.1
.7
.3
1
2, 3
8, 9
4, 5
6, 7
10, 11
12, 13
5, 7, 9
11
13
12
10
3
8
6
4
2

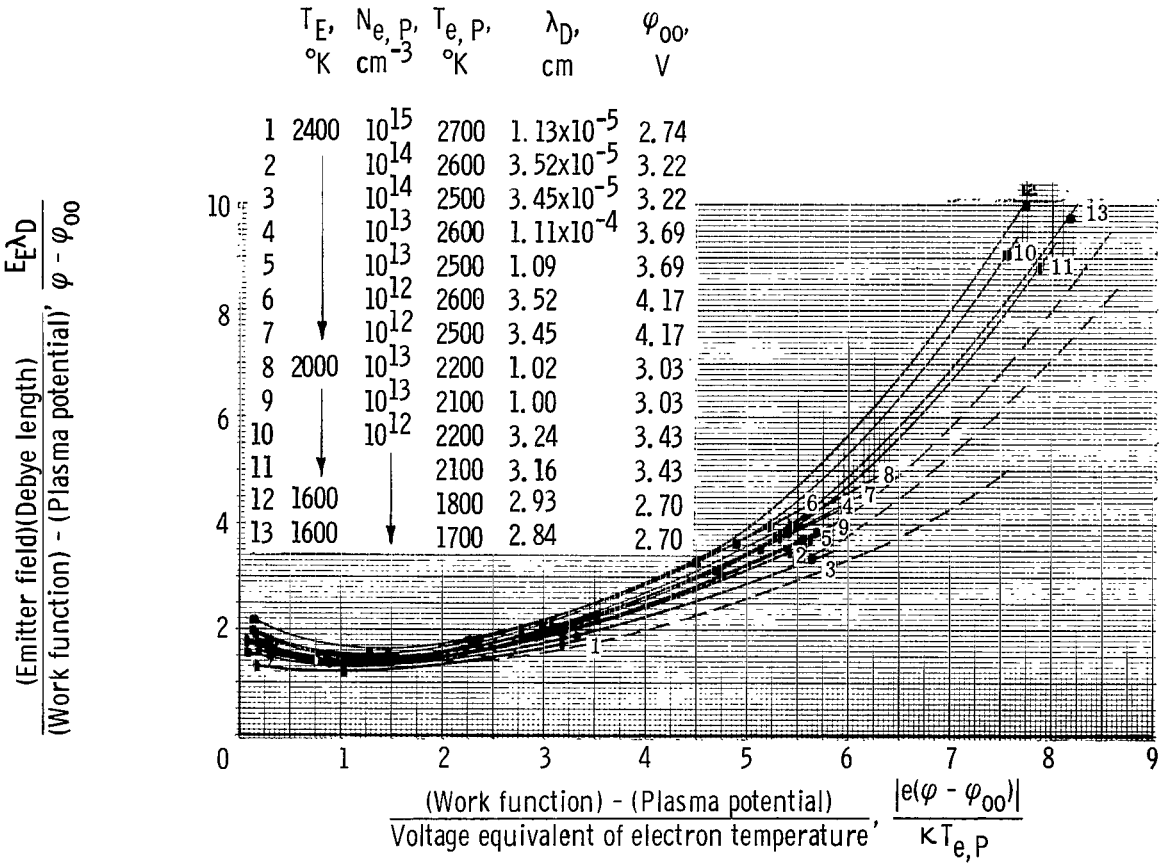

(b) Electron ($\varphi < \varphi_{oo}$) sheaths.

Figure 4. - Concluded.

Overall sheath voltage drop / (Work function) - (Plasma potential), $\frac{\Delta V_s}{\varphi - \varphi_{oo}}$
Sheath width / Debye length, $\frac{X_s}{\lambda_D}$
2.6
2.4
2.2
2.0
1.8
1.0
.9
.8

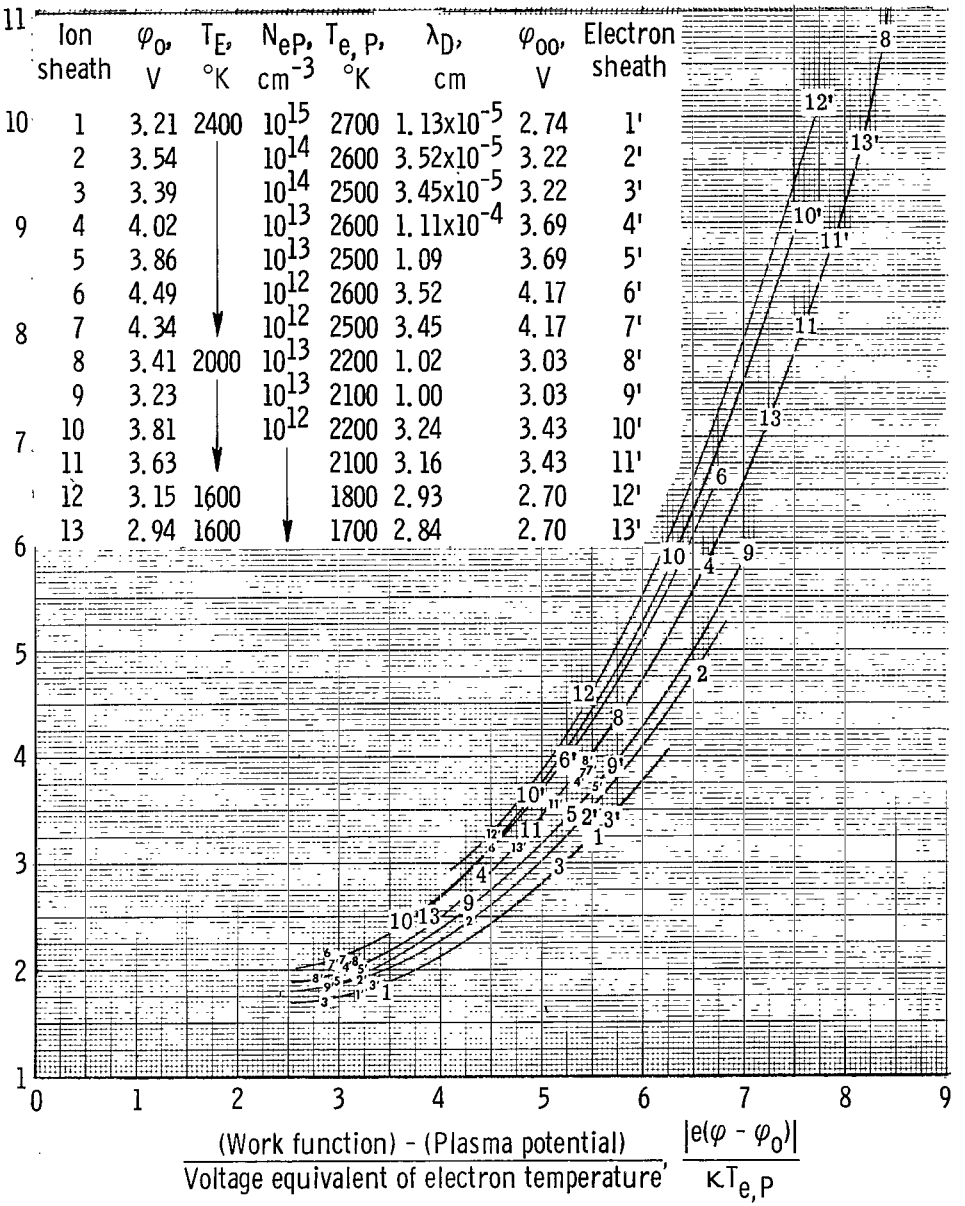

Figure 5. - Near-equilibrium ($T_{e,P} > T_E = T_{i,P} = T_{a,P}$) collisionless ion ($\varphi > \varphi_0$) and electron ($\varphi < \varphi_{00}$) sheaths.

Dimensionless sheath drop, $\frac{\Delta V_s}{\varphi - \varphi_\infty}$
1.0
.8
.6
.4
Sheath width / Emission Debye length, $\frac{X_s}{\lambda_{DE}}$
2.7
2.3
1.9
1.5
1.1
.7
.3

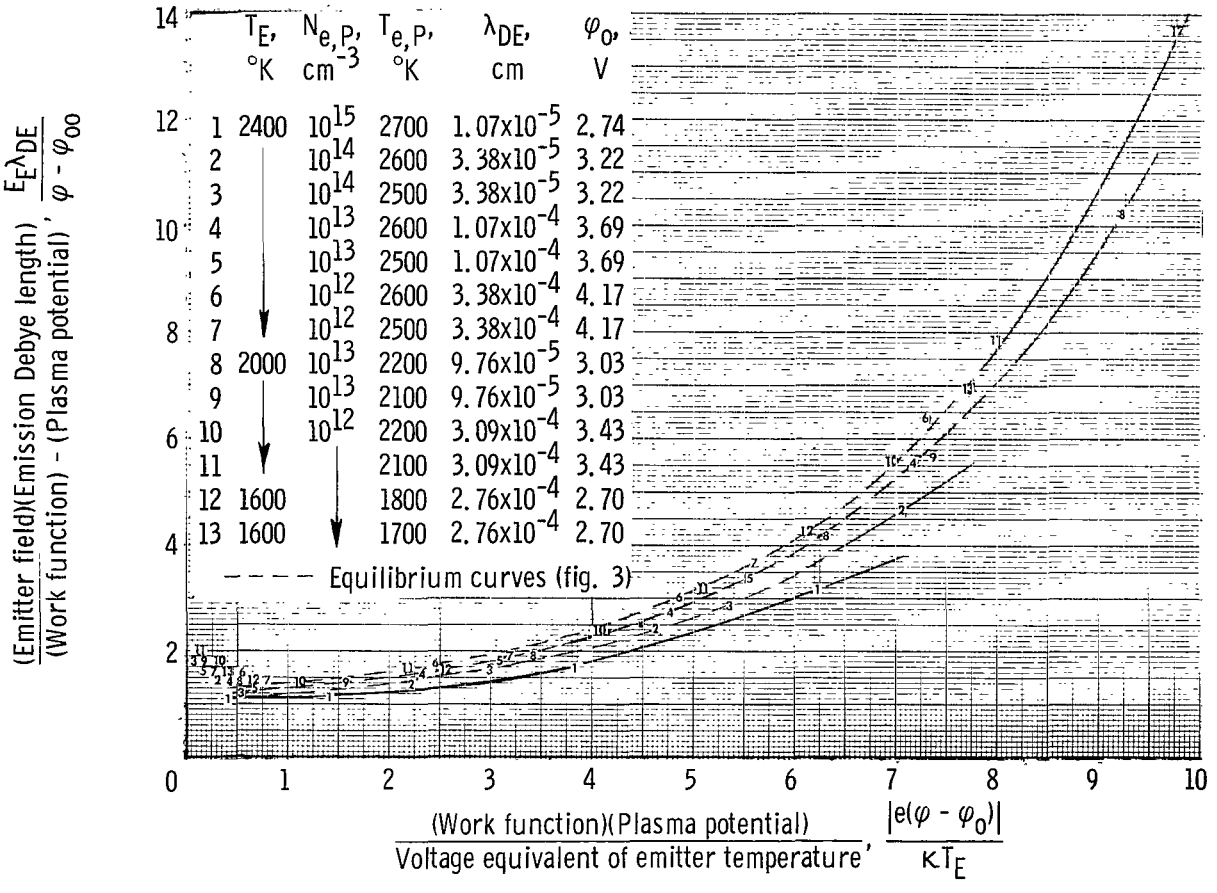

(a) Ion ($\varphi > \varphi_0$) sheaths.

Figure 6. - Nonequilibrium ($T_{e,P} > T_E = T_{i,P} = T_{a,P}$) collisionless sheaths (related to emission Debye length).

Sheath width / Emission Debye length, $\frac{X_s}{\lambda_{DE}}$
Overall sheath voltage drop / (Work function) - (Plasma potential), $\frac{\Delta V_s}{\phi - \phi_{oo}}$
T_E, °K
$N_{e,P}$, cm^{-3}
$T_{e,P}$, °K
λ_{DE}, cm
φ_{oo}, V
1 2400 10^{15} 2700 1.07×10^{-5} 2.74
2 10^{14} 2600 3.38×10^{-5} 3.22
3 10^{14} 2500 3.38×10^{-5} 3.22
4 10^{13} 2600 1.07×10^{-4} 3.69
5 10^{13} 2500 1.07×10^{-4} 3.69
6 10^{12} 2600 3.38×10^{-4} 4.17
7 10^{12} 2500 3.38×10^{-4} 4.17
8 2000 10^{13} 2200 9.76×10^{-5} 3.03
9 10^{13} 2100 9.76×10^{-5} 3.03
10 10^{12} 2200 3.09×10^{-4} 3.43
11 2100 3.09×10^{-4} 3.43
12 1600 1800 2.76×10^{-4} 2.70
13 1600 1700 2.76×10^{-4} 2.70
---- Equilibrium curves (fig. 3)

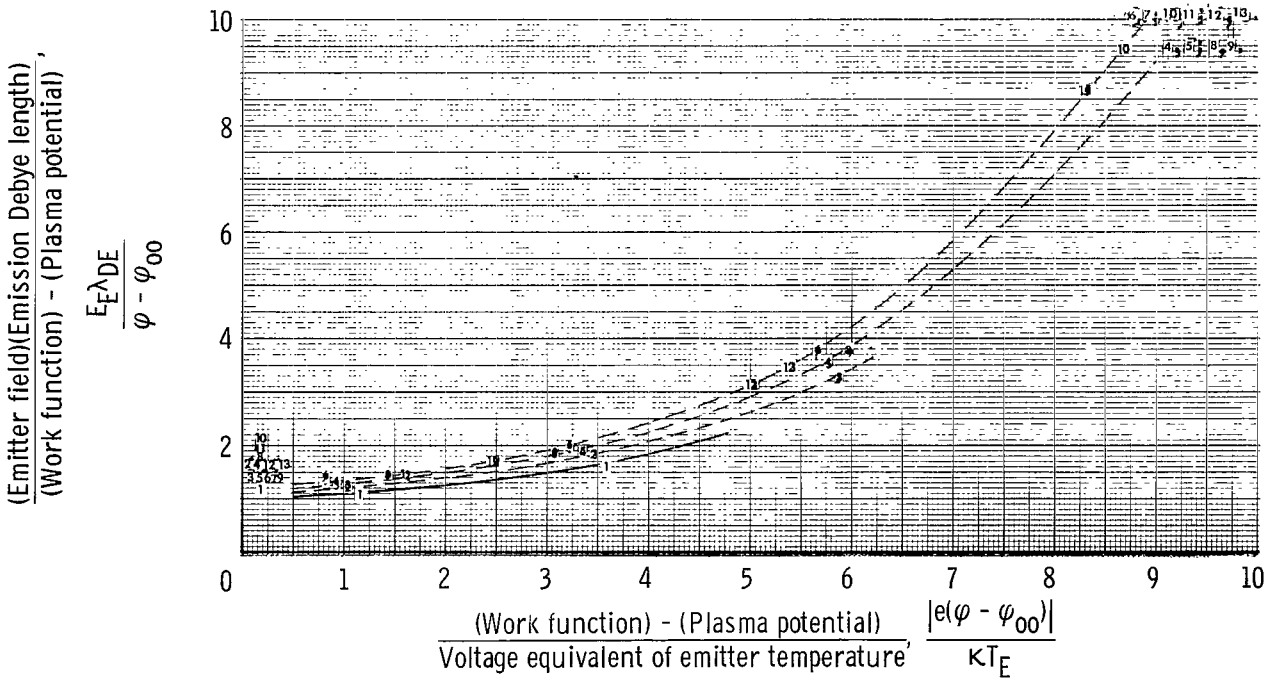

(b) Electron ($\varphi < \varphi_{oo}$) sheaths.

Figure 6. - Concluded.

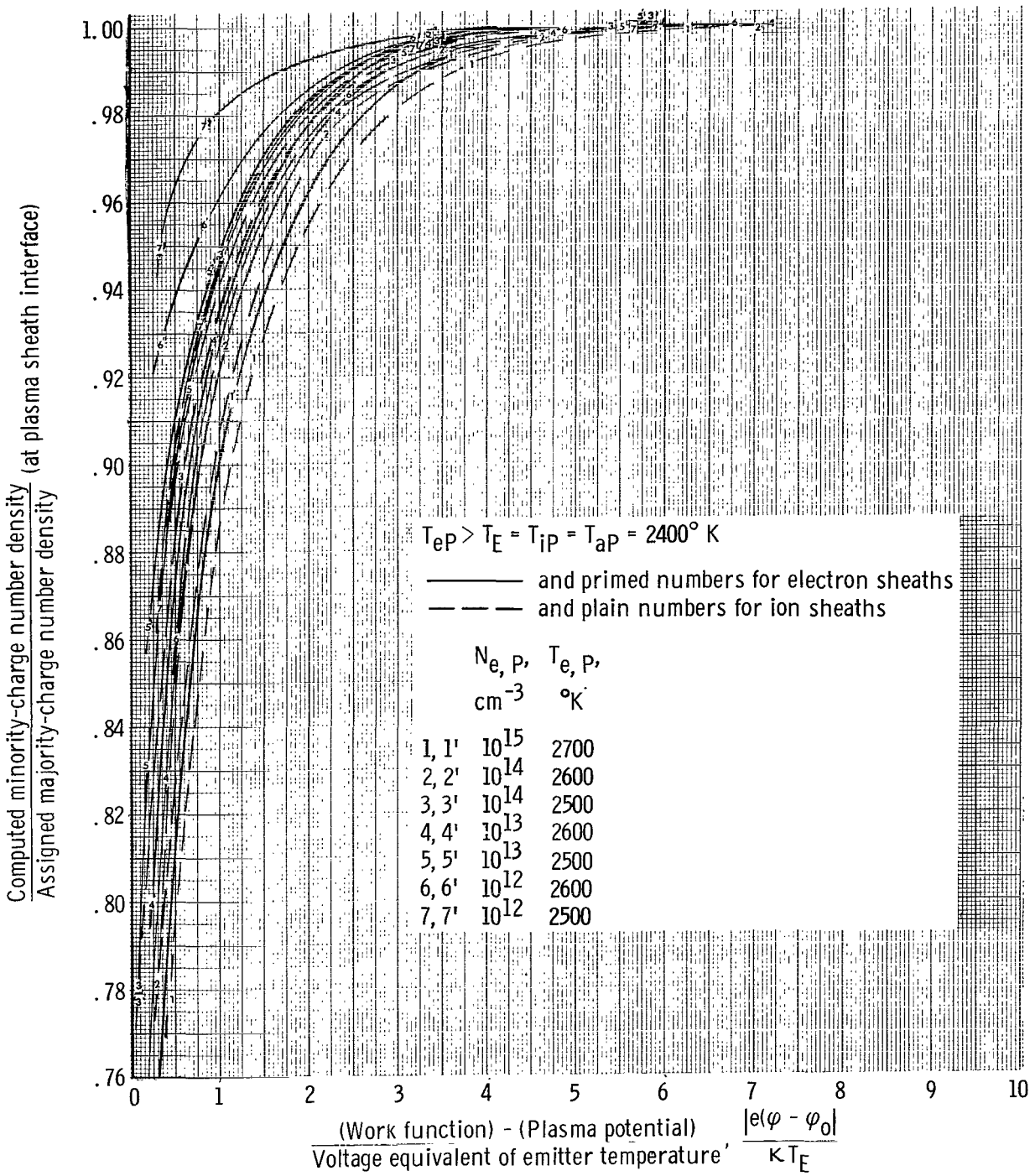

Figure 7. - Examples of charge imbalances at nonequilibrium cesium plasma sheath interfaces.

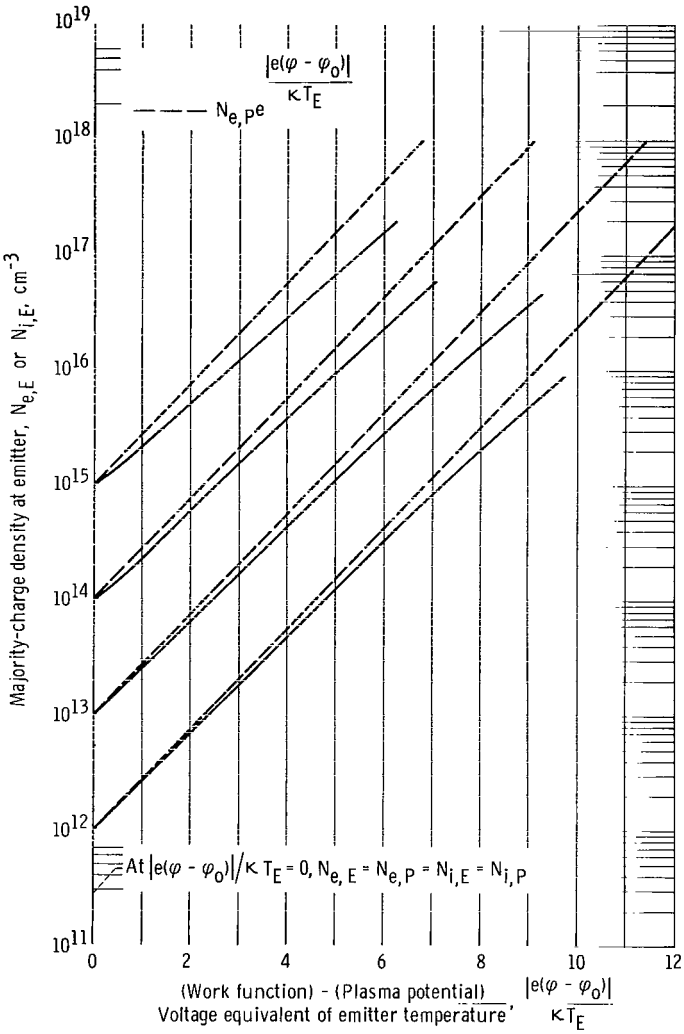

Figure 8. - Emitter charge densities in cesium plasmas. (All equilibrium and nonequilibrium data for ion and electron sheaths are included.)

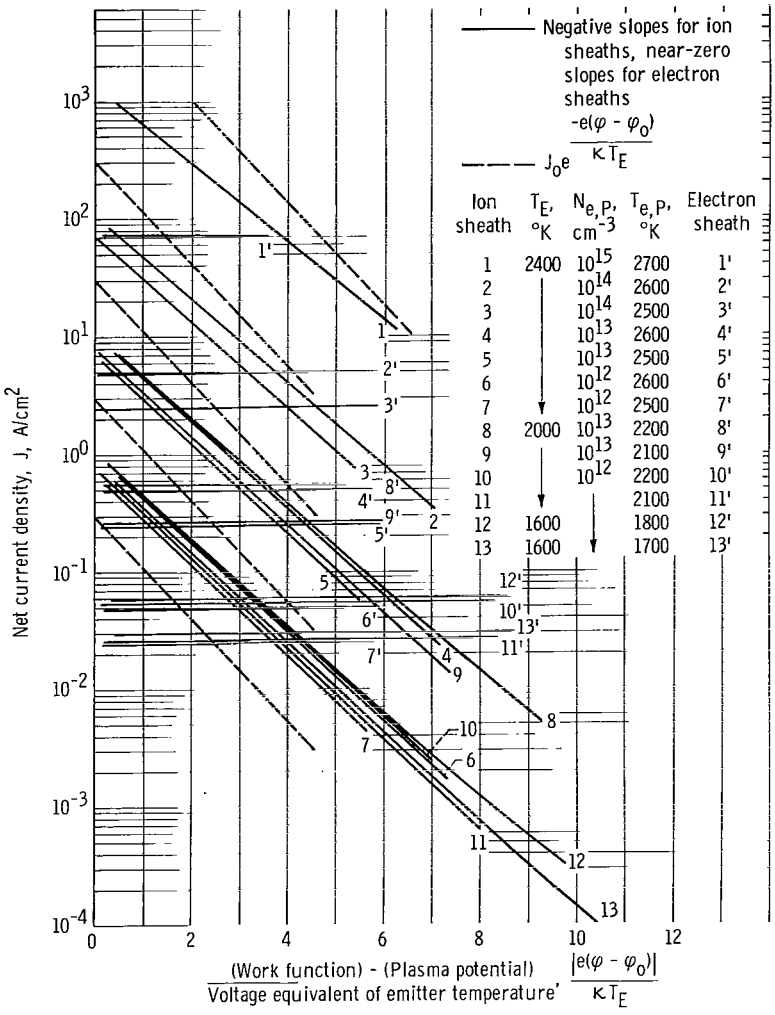

Figure 9. - Some sheath effects on charge transport between emitters and cesium plasmas.

SCHOTTKY

I = 3.893 TE = 2000. PHI = 3.100 NEP = 1.00E 13 TEP = 2.00E 03 TIP = 2000.0 LAMBDA = 9.7556E-05

PV = 8.283512E C4 LAMBDA(TE) = 9.7556E-05

CV	ND(CV)	NE(CV)	NI(CV)	E(CV)	X(CV)
0.	0.	9.9977782E 12	-1.000000E 13	-0.	2.457657E-04
0.00295	-3.449581E 11	9.827867E 12	-1.017283E 13	4.2966C90E C1	2.113970E-04
0.00591	-6.677999E 11	9.660837E 12	-1.034864E 13	8.5855E9E C1	1.5983C8E-04
0.00886	-1.030844E 12	9.496643E 12	-1.052749E 13	1.2871111E C2	1.311618E-04
0.01181	-1.374192E 12	9.335236E 12	-1.070943E 13	1.715642E C2	1.110842E-04
0.01477	-1.717944E 12	9.176569E 12	-1.089451E 13	2.1442253E C2	9.559214E-05
0.01772	-2.0622C2E 12	9.02C595E 12	-1.108280E 13	2.5725959E C2	8.296778E-05
0.02067	-2.407C67E 12	8.867269E 12	-1.127434E 13	3.0015521E C2	7.231077E-05
0.02362	-2.752640E 12	8.716544E 12	-1.146918E 13	3.4311C56E C2	6.308886E-05
0.02658	-3.099023E 12	8.568376E 12	-1.166740E 13	3.86C437E C2	5.496078E-05
0.02953	-3.446315E 12	8.422722E 12	-1.186904E 13	4.2900C99E C2	4.769440E-05
0.03248	-3.794630E 12	8.279538E 12	-1.207417E 13	4.720C73E C2	4.112459E-05
0.03544	-4.144058E 12	8.138781E 12	-1.228284E 13	5.15C393E C2	3.512966E-05
0.03839	-4.494708E 12	8.000409E 12	-1.249512E 13	5.581C91E C2	2.961731E-05
0.04134	-4.846683E 12	7.864380E 12	-1.271106E 13	6.0121598E C2	2.451591E-05
0.04430	-5.2C0090E 12	7.730653E 12	-1.293074E 13	6.443747E C2	1.976867E-05
0.04725	-5.555C33E 12	7.599184E 12	-1.315422E 13	6.8757771E C2	1.532989E-05
0.05020	-5.911624E 12	7.469931E 12	-1.338155E 13	7.3083C1E C2	1.116217E-05
0.05315	-6.269976E 12	7.342846E 12	-1.361282E 13	7.7413270E C2	7.234557E-06
0.05611	-6.630220E 12	7.217865E 12	-1.384808E 13	8.175C13E C2	3.521141E-06
0.05906	-6.992739E 12	7.094675E 12	-1.408741E 13	8.6092722E C2	0.

JEE	= 7.8501111E 00	JEP	= 1.112723E 01	JIP	= 2.260730E-02	JAP	= 6.764668E 00
J	= -6.5514135E-03	PP	= 6.238256E-01	JIE	= 3.184783E-02	JAE	= 6.764668E 00
JA	= 5.9664664E-06	JI	= -1.625815E-09	JE	= -8.591473E-03	JA/JAP	= 8.81C510E-09
JE/JEP	= -7.7211126E-04	JI/JIP	= -7.2C95241E-08	UVS	= 0.05906	XCVS	= 2.457657E-04
NAP	= 2.992338E 15	XD/LAM	= 2.515231E 00	SC	= 1.113828E-02	PPZ	= 3.02551
EDVS	= 6.6C52722E 02	DVSRD	= 7.0C9217E-02			CVS/RC	= 8.422C96E-01
ELM/RD	= 1.156258E 0C	PHZZ	= 3.02572CE 00			CRC/KT	= 4.C67C87E-01
NTP	= 3.012338E 15	NCE	= 2.118209E 13	NTE	= 3.013520E 15	RC/KTE	= 4.C67C87E-01
X/LMTE	= 2.515231E 00	ELT/RD	= 1.158258E 00	NEPA	= 9.997782E 12		

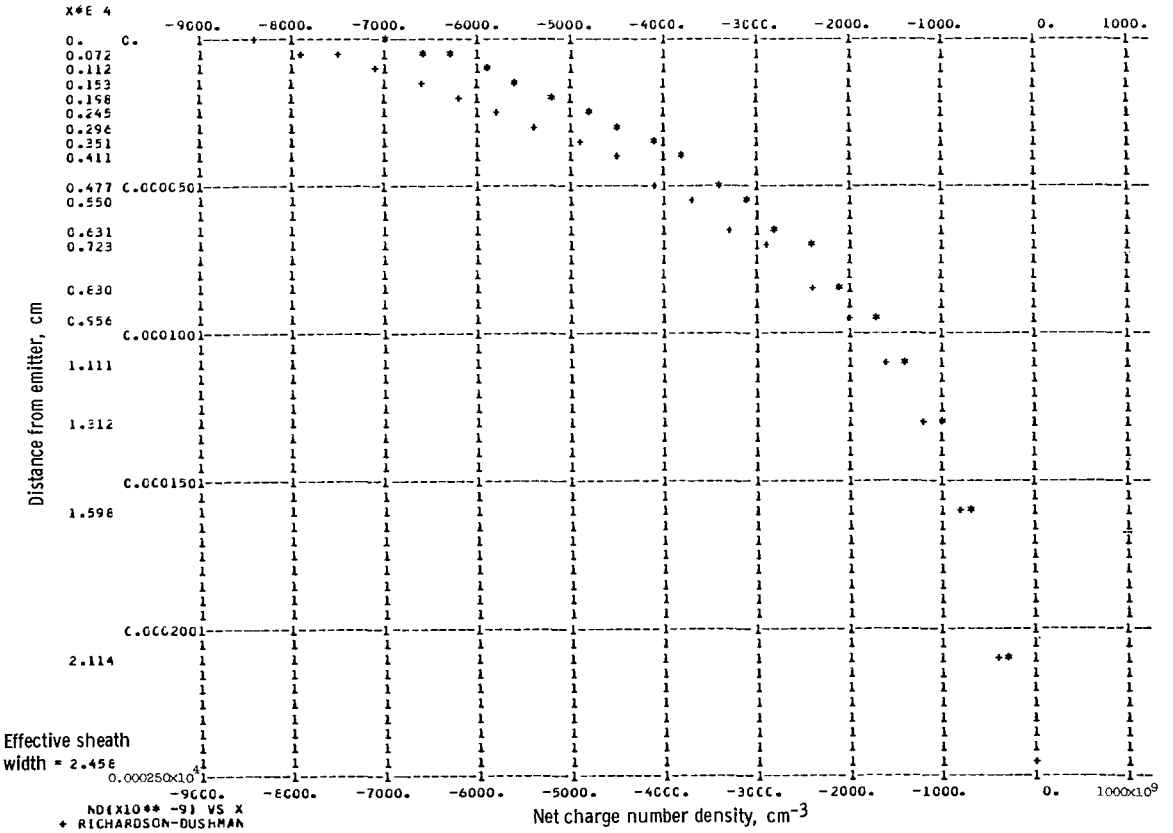

(a) Work function, $\varphi = 3.10$.

Figure 10. - Plane ion sheaths between emitters and cesium plasmas at equilibrium.

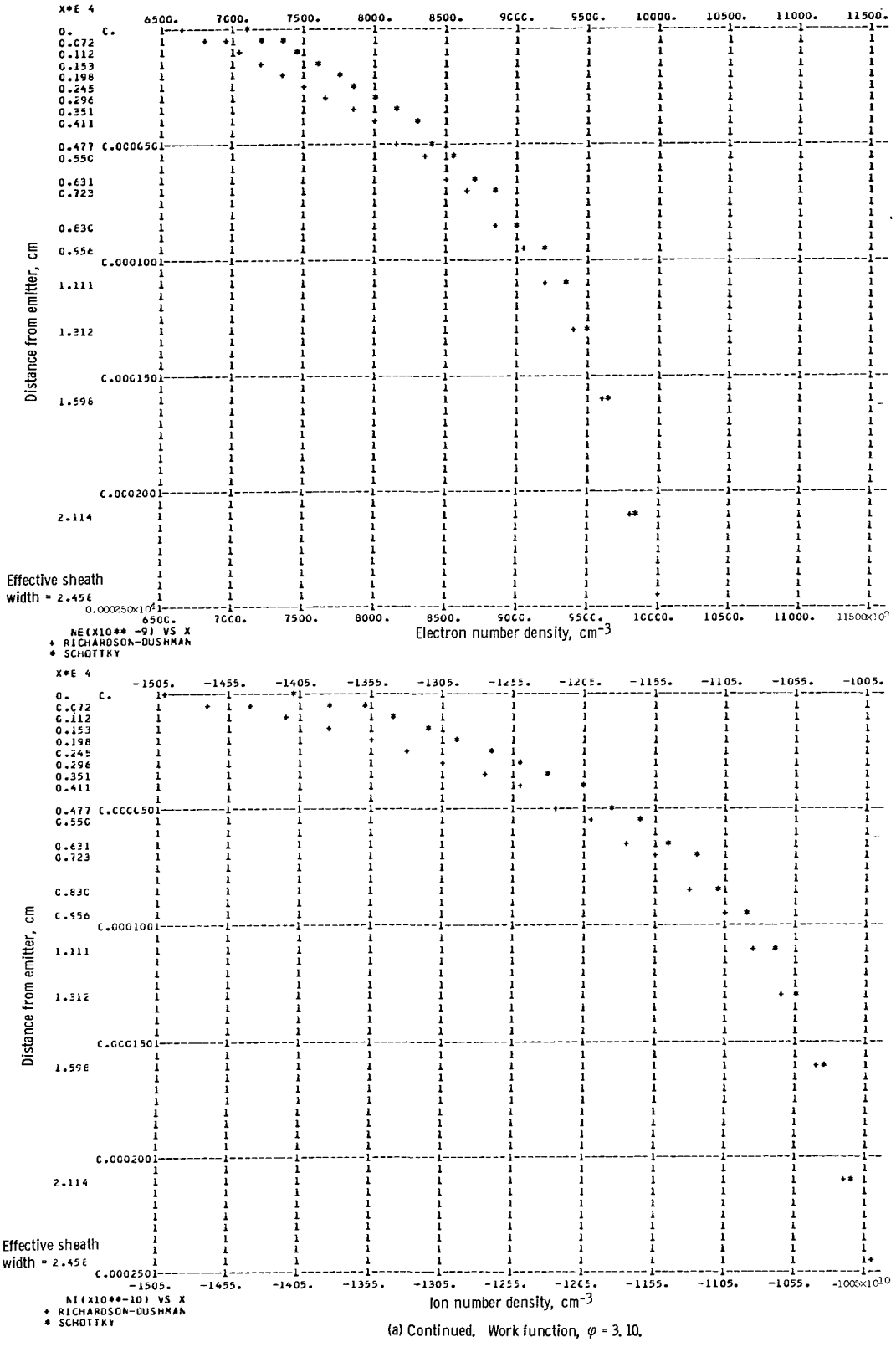

(a) Continued. Work function, φ = 3. 10.

Figure 10. - Continued.

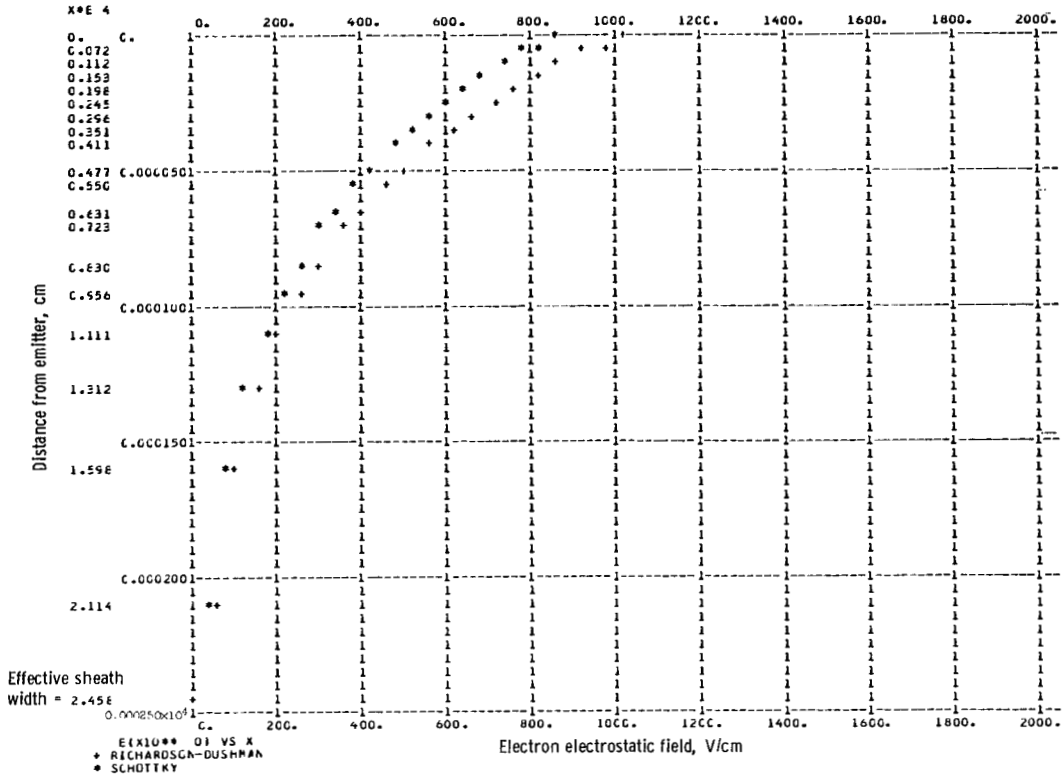

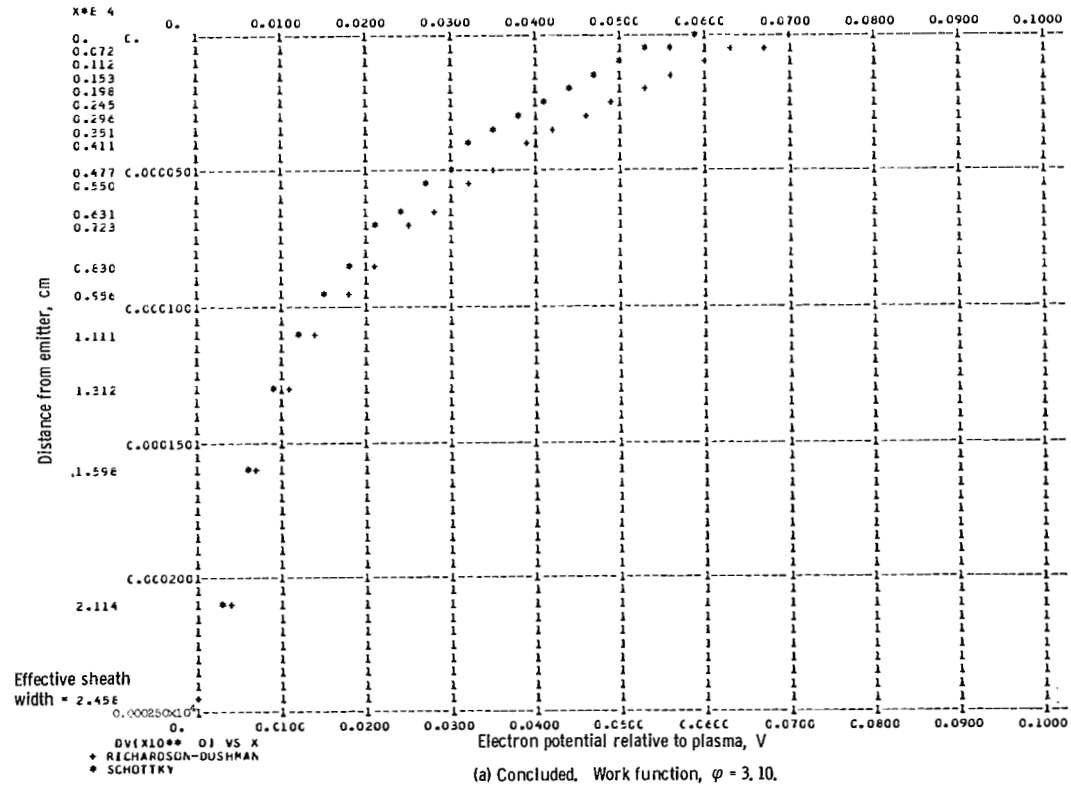

(a) Concluded. Work function, $\varphi = 3.10$.

Figure 10. - Continued.

SCHOTTKY

I = 3.893 TE = 2000. PHI = 4.500 NEP = 1.00E 13 TEP = 2.00E 03 TIP = 2000.0 LAMBDA = 9.7556E-05

PV = 8.283512E 04 LAMBDA(TE) = 9.7556E-05

DV	ND(DV)	NE(DV)	NI(DV)	E(DV)	X(DV)
0.	0.	9.999999E 12	-1.000000E 13	-0.	1.964045E-04
0.06715	-7.991031E 12	6.773149E 12	-1.476418E 13	9.859681E 02	1.623539E-04
0.13429	-1.721055E 13	4.587555E 12	-2.179810E 13	2.009514E 03	1.115961E-04
0.20144	-2.907588E 13	3.107220E 12	-3.218310E 13	3.109543E 03	8.409154E-05
0.26859	-4.541114E 13	2.104567E 12	-4.751571E 13	4.327955E 03	6.553769E-05
0.33573	-6.872759E 13	1.425454E 12	-7.015305E 13	5.711137E 03	5.195175E-05
0.40288	-1.026097E 14	9.654815E 11	-1.035752E 14	7.311746E 03	4.143144E-05
0.47003	-1.522664E 14	6.539350E 11	-1.529203E 14	9.195726E 03	3.318676E-05
0.53718	-2.253313E 14	4.429198E 11	-2.257742E 14	1.141595E 04	2.659380E-05
0.60432	-3.330371E 14	2.999960E 11	-3.333371E 14	1.408322E 04	2.126988E-05
0.67147	-4.919417E 14	2.031916E 11	-4.921449E 14	1.728301E 04	1.694338E-05
0.73862	-7.264739E 14	1.376245E 11	-7.266115E 14	2.114077E 04	1.341272E-05
0.80576	-1.072689E 15	9.321492E 10	-1.072782E 15	2.580339E 04	1.052350E-05
0.87291	-1.583812E 15	6.313563E 10	-1.583875E 15	3.144836E 04	8.154806E-06
0.94006	-2.338418E 15	4.276245E 10	-2.338461E 15	3.829026E 04	6.210426E-06
1.00720	-3.452517E 15	2.896337E 10	-3.452546E 15	4.655055E 04	4.613015E-06
1.07435	-5.097381E 15	1.961702E 10	-5.097400E 15	5.666433E 04	3.299914E-06
1.14150	-7.525879E 15	1.328655E 10	-7.525892E 15	6.889533E 04	2.220109E-06
1.20864	-1.111135E 16	8.998760E 09	-1.111136E 16	8.374523E 04	1.331920E-06
1.27579	-1.640501E 16	6.094447E 09	-1.640501E 16	1.017515E 05	6.012160E-07
1.34294	-2.422065E 16	4.126464E 09	-2.422065E 16	1.237091E 05	0.

JEE	= 4.5651C9E-03	JEP	= 1.112723E 01	JIP	= 2.260730E-02	JAP	= 6.764668E 00
J	= -4.9564C8E-06	PP	= 6.238256E-01	JIE	= 5.475637E 01	JAE	= 6.764668E 00
JA	= 5.966464E-08	JI	= -1.356984E-09	JE	= -4.997011E-06	JA/JAP	= 8.810510E-09
JE/JEP	= -4.49C756E-07	JI/JIP	= -6.179349E-08	DVS	= 1.34294	XDVS	= 1.564045E-04
NAP	= 2.952338E 15	XD/LAM	= 2.013252E 00	SC	= 1.335168E-01	PHZ	= 3.02591
EDVS	= 1.237051E 05	DVSRD	= 1.470092E 00			EVS/RD	= 9.135061E-01
ELM/RD	= 8.209383E 00	PHZZ	= 3.029720E 00			ERC/KT	= 8.533185E 00
NTP	= 3.012338E 15	NCE	= 2.422066E 16	NTE	= 2.721299E 16	RC/KTE	= 8.533185E 00
X/LMTE	= 2.013252E 00	ELT/RD	= 8.209383E 00	NEPA	= 9.999999E 12		

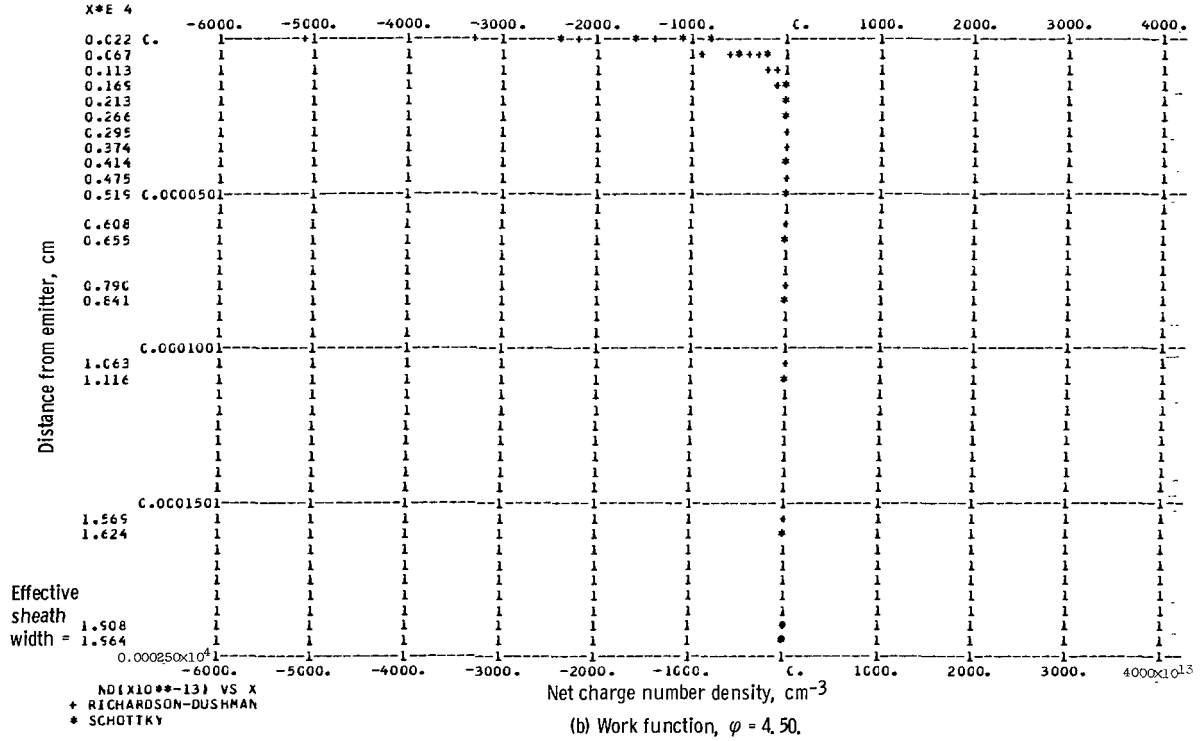

(b) Work function, φ = 4.50.

Figure 10. - Continued.

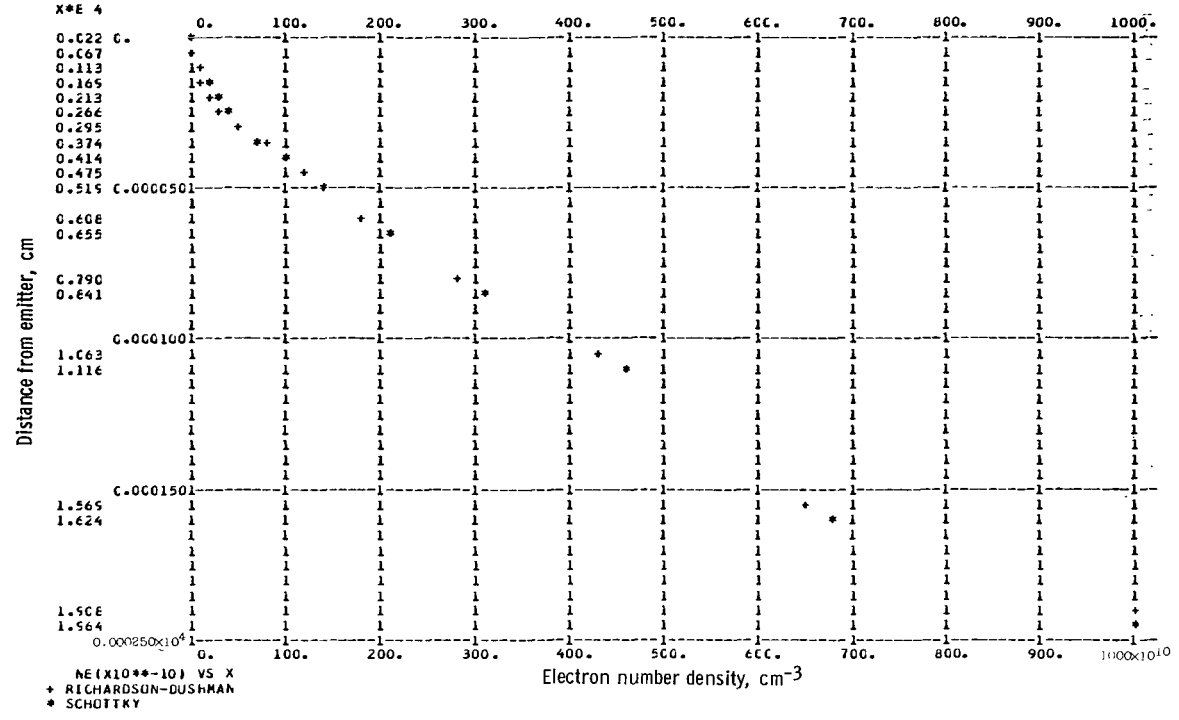

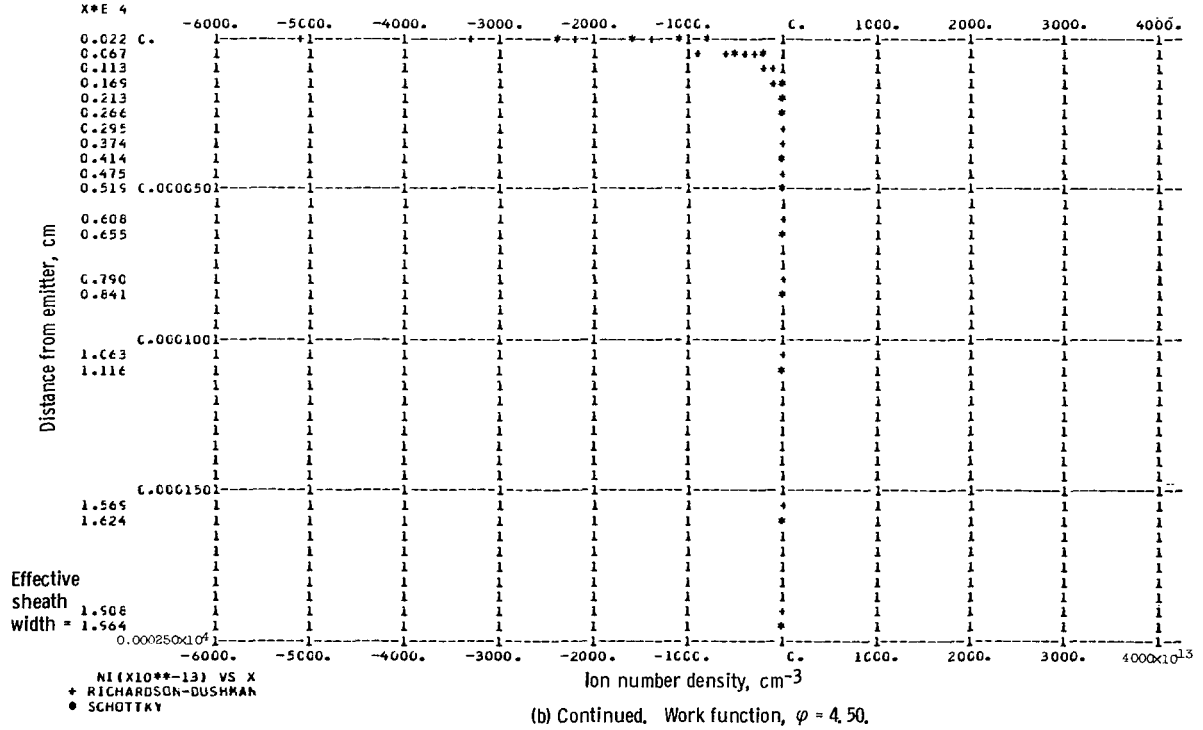

(b) Continued. Work function, $\varphi = 4.50$.

Figure 10. - Continued.

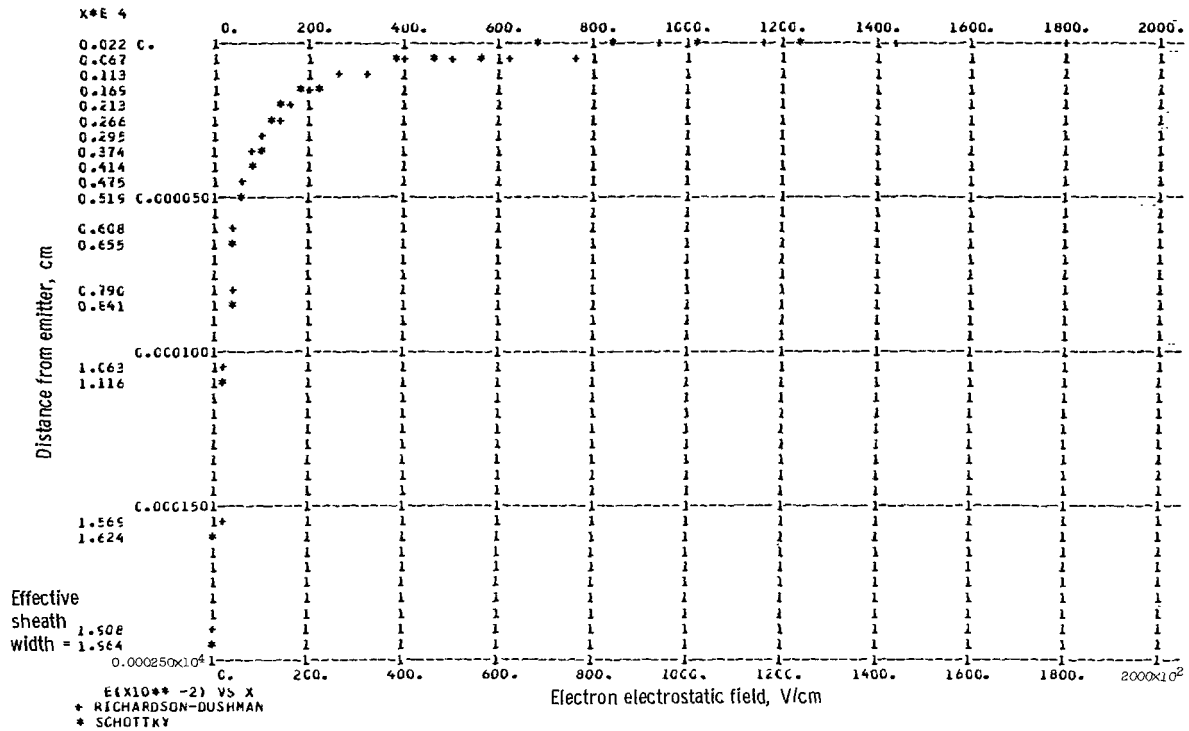

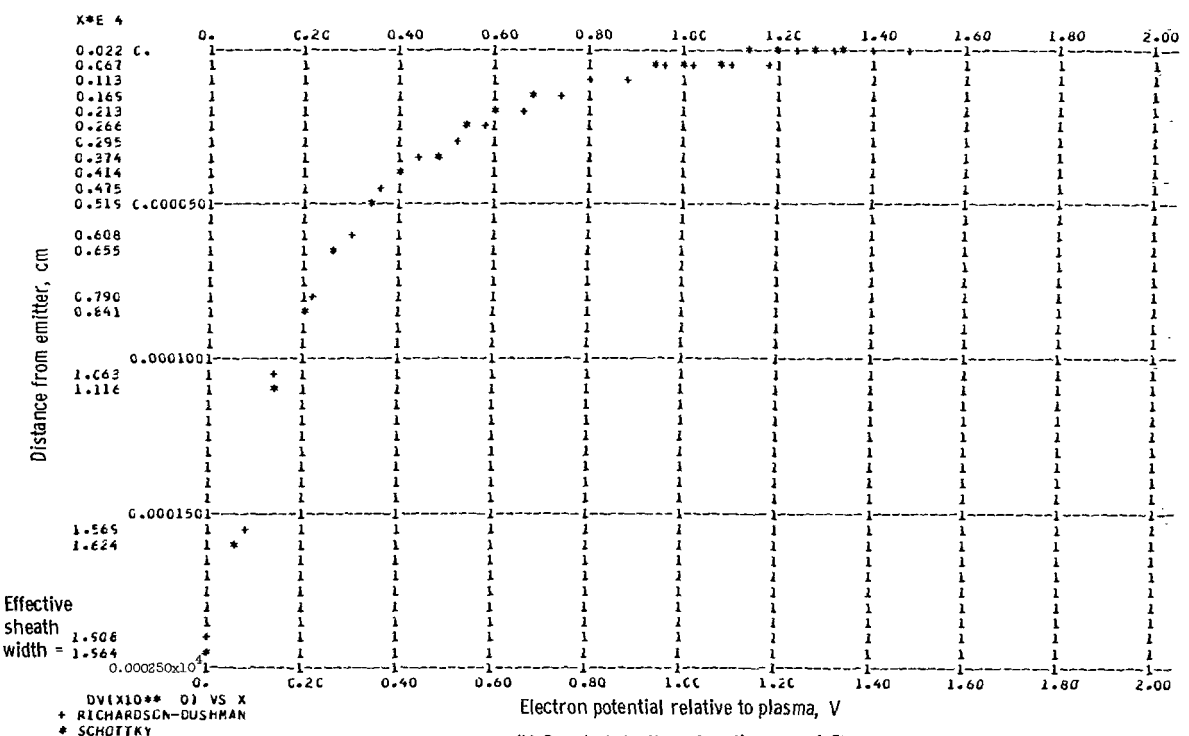

(b) Concluded. Work function, φ = 4.50.

Figure 10. - Concluded.

SCHOTTKY

I = 3.893 TE = 2000. PHI = 4.000 NEP = 1.00E 13 TEP = 2.20E 03 TIP = 2000.0 LAMBDA = 1.0232E-04

PV = 8.283512E 04 LAMBDA(TE) = 5.7556E-05

DV	ND(DV)	NE(DV)	NI(DV)	E(DV)	X(DV)
0.	0.	9.926573E 12	-1.000000E 13	-0.	2.350967E-04
0.02752	-3.157793E 12	8.573747E 12	-1.173154E 13	3.966158E 02	2.004182E-04
0.05504	-6.359476E 12	7.403426E 12	-1.376290E 13	7.955093E 02	1.484304E-04
0.08257	-9.755084E 12	6.390922E 12	-1.614601E 13	1.198161E 03	1.196361E-04
0.11009	-1.342687E 13	5.514880E 12	-1.894175E 13	1.605963E 03	9.962951E-05
0.13761	-1.746477E 13	4.756824E 12	-2.222159E 13	2.032722E 03	8.428508E-05
0.16513	-2.196856E 13	4.100771E 12	-2.606935E 13	2.469473E 03	7.194290E-05
0.19265	-2.705047E 13	3.532889E 12	-3.058336E 13	2.922777E 03	6.166227E-05
0.22018	-3.283779E 13	3.041208E 12	-3.587900E 13	3.395429E 03	5.290128E-05
0.24770	-3.947623E 13	2.619360E 12	-4.209159E 13	3.890355E 03	4.531128E-05
0.27522	-4.713355E 13	2.246365E 12	-4.937991E 13	4.410629E 03	3.865411E-05
0.30274	-5.600381E 13	1.926434E 12	-5.793024E 13	4.955493E 03	3.275947E-05
0.33026	-6.631230E 13	1.648798E 12	-6.796110E 13	5.540283E 03	2.750104E-05
0.35779	-7.832128E 13	1.407559E 12	-7.972883E 13	6.156545E 03	2.278224E-05
0.38531	-9.233665E 13	1.197550E 12	-9.353420E 13	6.813061E 03	1.852741E-05
0.41283	-1.087158E 14	1.014189E 12	-1.097300E 14	7.512872E 03	1.467596E-05
0.44035	-1.278769E 14	8.533204E 11	-1.287302E 14	8.260EC5E 03	1.117849E-05
0.46787	-1.503094E 14	7.109723E 11	-1.510204E 14	9.061C61E 03	7.954067E-06
0.49540	-1.765873E 14	5.828181E 11	-1.771701E 14	9.920345E 03	5.088315E-06
0.52292	-2.073856E 14	4.622140E 11	-2.078479E 14	1.084251E 04	2.431998E-06
0.55044	-2.435405E 14	2.970385E 11	-2.438376E 14	1.183408E 04	0.

JEE	= 5.066489E-02	JEP	= 1.167033E 01	JIP	= 2.260730E-02	JAP	= 7.521E43E-01
J	= -5.851718E-01	PP	= 7.325187E-02	JIE	= 5.512509E-01	JAE	= 7.521E43E-01
JA	= 0.	JI	= -6.984919E-10	JE	= -5.891718E-01	JA/JAP	= 0.
JE/JEP	= -5.048457E-02	JI/JIP	= -3.089675E-08	DVS	= 0.55044	XDVS	= 2.350967E-04
NAP	= 3.327175E 14	XD/LAM	= 2.297719E 00	SC	= 4.129545E-02	PHZ	= 3.4CE46
EDVS	= 1.1E34CEE 04	DVSKD	= 5.515444E-01			DVS/RD	= 9.3C5128E-01
ELM/RD	= 2.046900E 0C	PHZZ	= 3.02572CE 00			GRD/KT	= 3.120388E 00
NTP	= 3.527175E 14	NCE	= 2.441346E 14	NTE	= 5.768521E 14	RD/KTE	= 3.432427E CC
X/LMTE	= 2.4C9866E 0C	ELT/RD	= 1.951642E 00	NEPA	= 9.926573E 12		

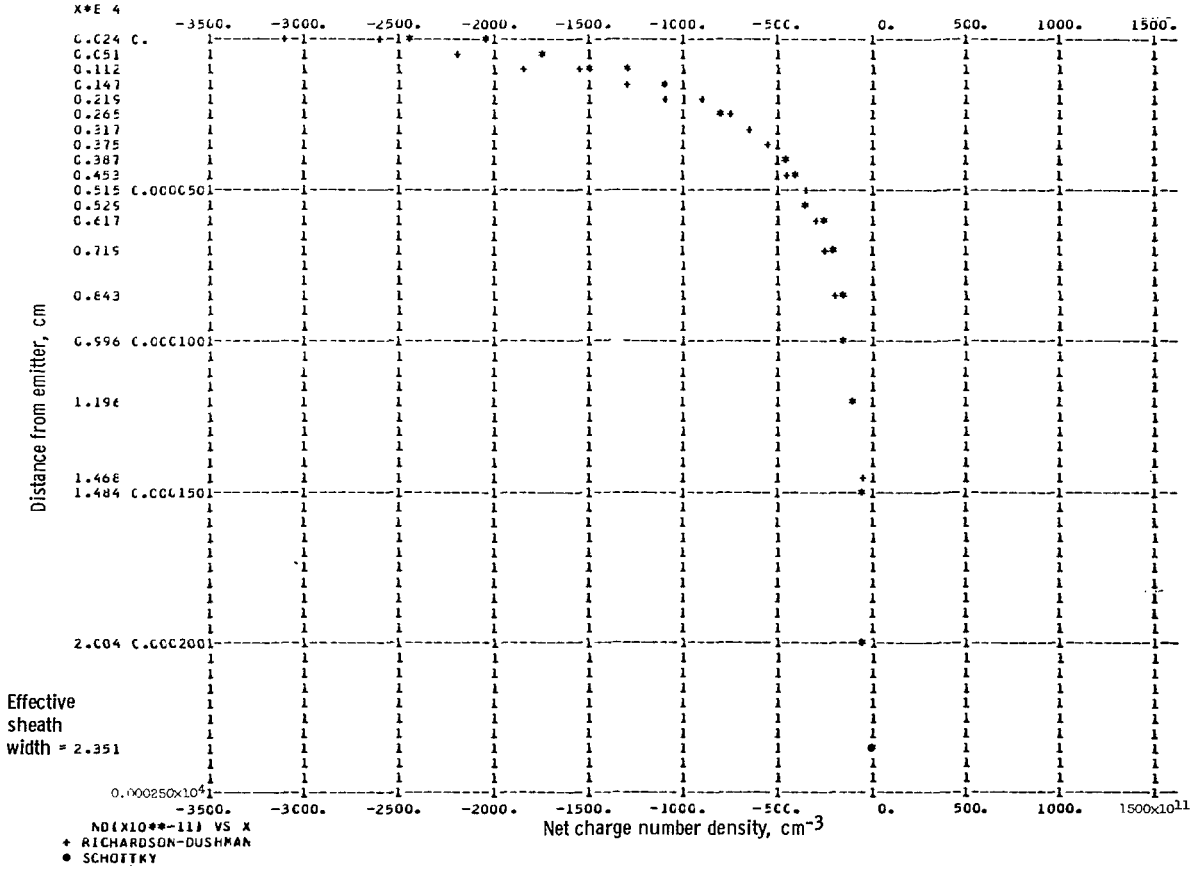

Figure 11. - Plane ion sheath between an emitter and a cesium plasma near equilibrium.

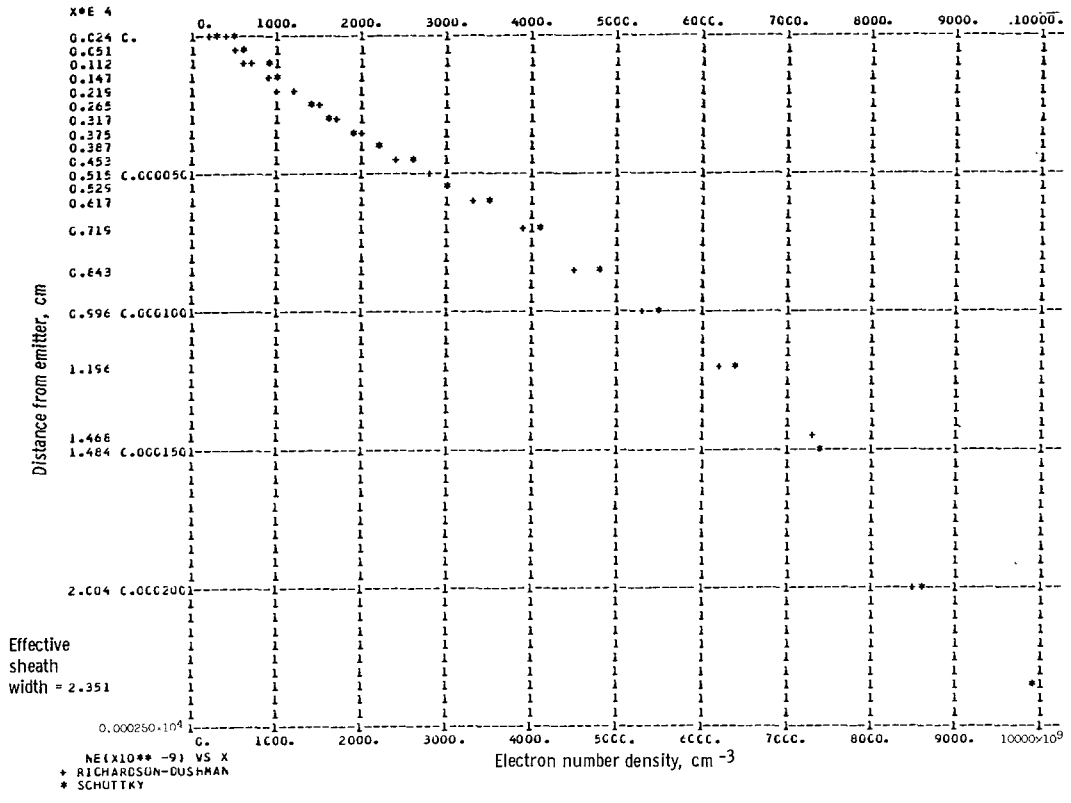

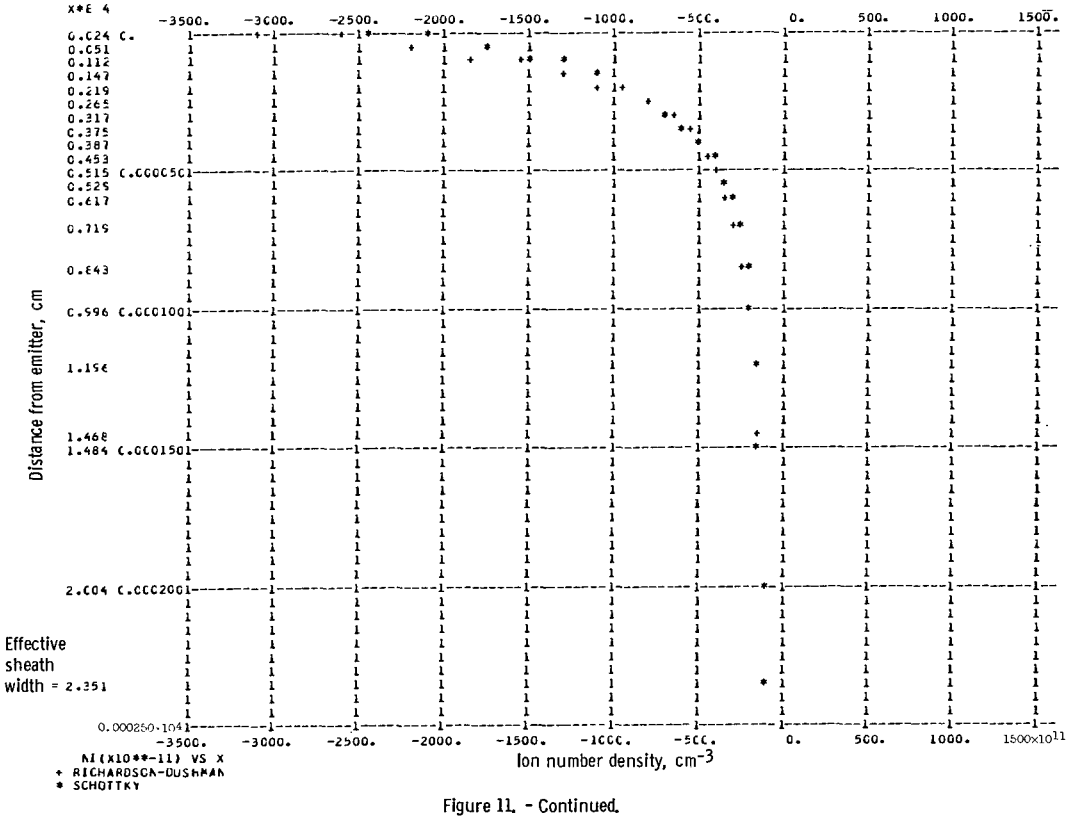

Figure 11. - Continued.

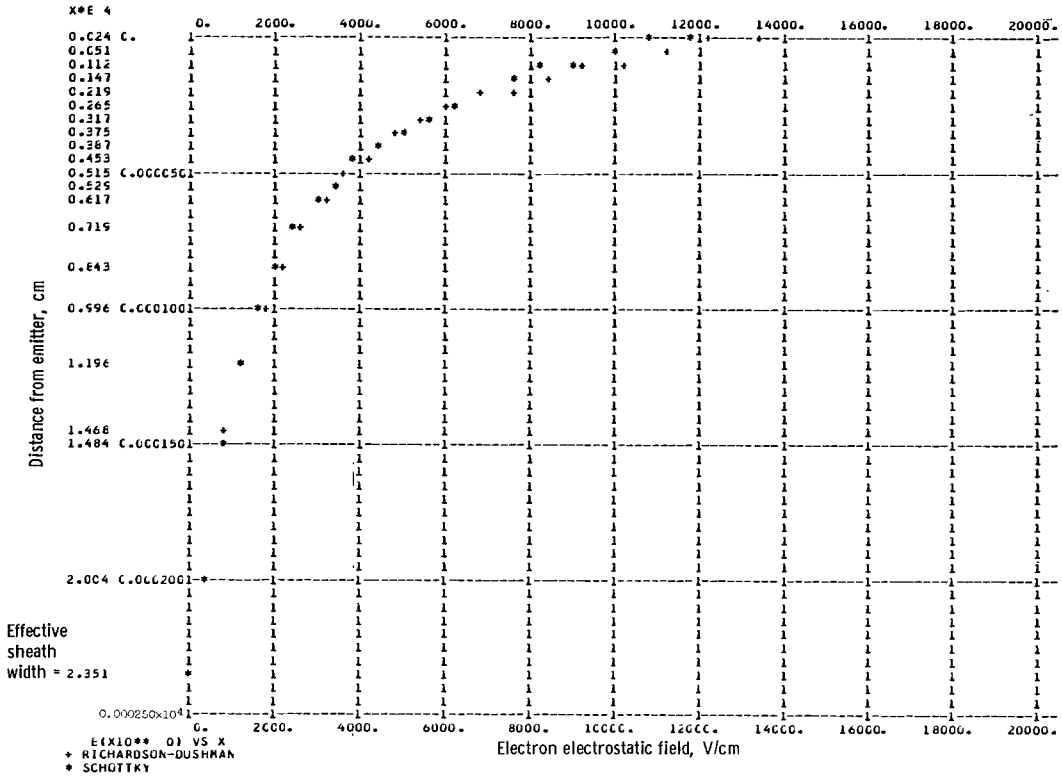

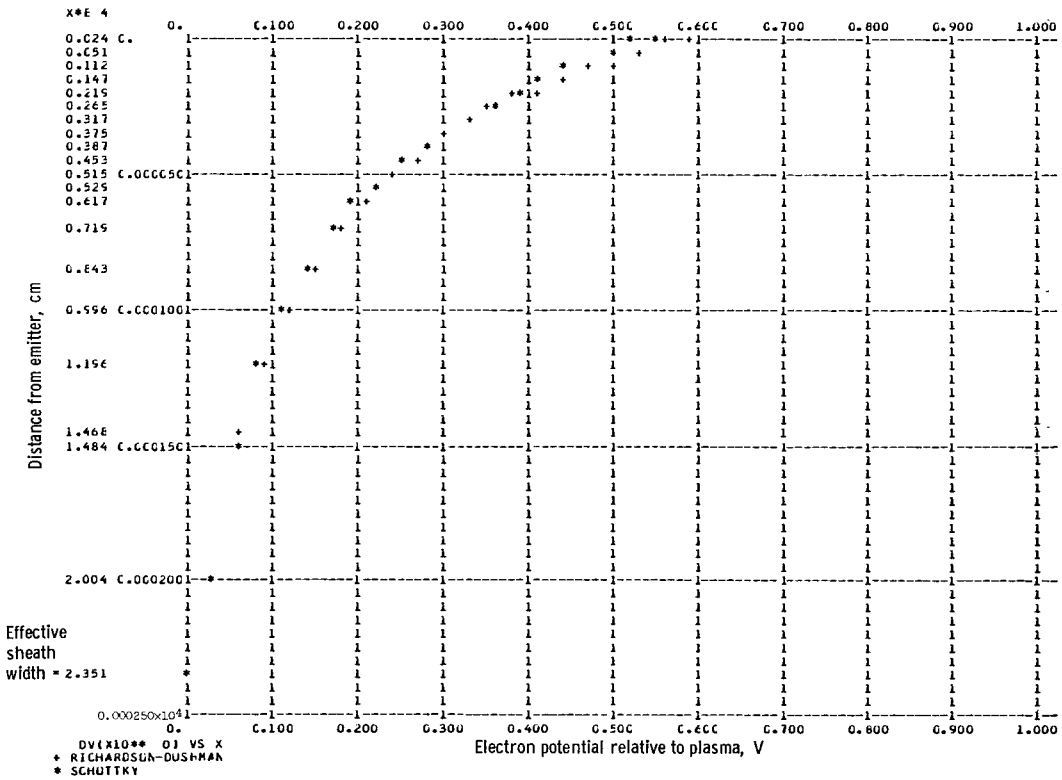

Figure 11. - Concluded.

SCHOTTKY

I = 3.893 TE = 2000. PHI = 2.500 NEP = 1.00E 13 TEP = 2000.0 TIP = 2000.0 LAMBDA = 9.7556E-05

PV = 8.283512E 04 LAMBDA(TE) = 9.7556E-05

DV	ND(DV)	NE(DV)	NI(DV)	E(DV)	X(DV)
0.	0.	1.000000E 13	-9.999908E 12	0.	2.356904E-04
-0.02461	2.865986E 12	1.153509E 13	-8.669105E 12	-3.574906E 02	2.012676E-04
-0.04522	5.790427E 12	1.330583E 13	-7.515405E 12	-7.168018E 02	1.496771E-04
-0.07383	8.833159E 12	1.534840E 13	-6.515240E 12	-1.079767E 03	1.211127E-04
-0.09545	1.205634E 13	1.770452E 13	-5.648176E 12	-1.448246E 03	1.012189E-04
-0.12306	1.552582E 13	2.042232E 13	-4.896500E 12	-1.824C99E 03	8.597556E-05
-0.14767	1.931248E 13	2.355734E 13	-4.244857E 12	-2.2C9262E C3	7.365921E-05
-0.17228	2.349367E 13	2.717360E 13	-3.679934E 12	-2.605655E 03	6.336644E-05
-0.19689	2.815480E 13	3.134500E 13	-3.190191E 12	-3.015418E 03	5.456281E-05
-0.22150	3.339112E 13	3.615674E 13	-2.765621E 12	-3.440522E C3	4.690511E-05
-0.24612	3.930957E 13	4.170713E 13	-2.397553E 12	-3.883175E C3	4.015936E-05
-0.27073	4.603108E 13	4.810955E 13	-2.078466E 12	-4.345635E C3	3.415859E-05
-0.29534	5.369296E 13	5.549480E 13	-1.801842E 12	-4.830261E C3	2.877917E-05
-0.31995	6.245173E 13	6.401376E 13	-1.562030E 12	-5.339524E C3	2.392685E-05
-0.34456	7.248632E 13	7.384045E 13	-1.354131E 12	-5.876C24E C3	1.952795E-05
-0.36917	8.400174E 13	8.517563E 13	-1.173896E 12	-6.442455E 03	1.552360E-05
-0.39379	9.723322E 13	9.825087E 13	-1.017645E 12	-7.041628E C3	1.186597E-05
-0.41840	1.124511E 14	1.133333E 14	-8.821833E 11	-7.677C79E C3	8.515510E-06
-0.44301	1.299662E 14	1.307310E 14	-7.647426E 11	-8.351489E C3	5.439093E-06
-0.46762	1.501364E 14	1.507993E 14	-6.629189E 11	-9.068498E C3	2.608622E-06
-0.49223	1.733738E 14	1.739484E 14	-5.745706E 11	-9.831764E 03	0.

JEE	= 1.935564E 02	JEP	= 1.112723E 01	JIP	= 2.260730E-02	JAP	= 6.764668E 00
J	= 1.771114E-06	PP	= 6.238296E-01	JIE	= 1.298242E-03	JAE	= 6.764670E 00
JA	= 1.43C511E-06	JI	= 1.413486E-06	JE	= 3.576279E-07	JA/JAP	= 2.114618E-07
JE/JEP	= 3.213989E-08	JI/JIP	= 6.252343E-05	DVS	= -0.49223	XDVS	= 2.356504E-04
NAP	= 2.952338E 15	XDLAM	= 2.415954E 00	SC	= 3.764010E-02	PHZ	= 3.02572
EDVS	= -5.831764E 02	DVSRD	= -5.257203E-01			DVS/RD	= 9.292320E-01
ELM/RD	= 1.81C665E 00	PHZZ	= 3.02572CE 00			DRD/KT	= 3.C73693E 00
NTP	= 3.012338E 15	NCE	= 1.745230E 14	NTE	= 3.166861E 15	RC/KTE	= -3.C73693E 00
X/LMTE	= 2.415954E 00	ELT/RD	= 1.81C665E 00	NIPA	= -9.999908E 12		

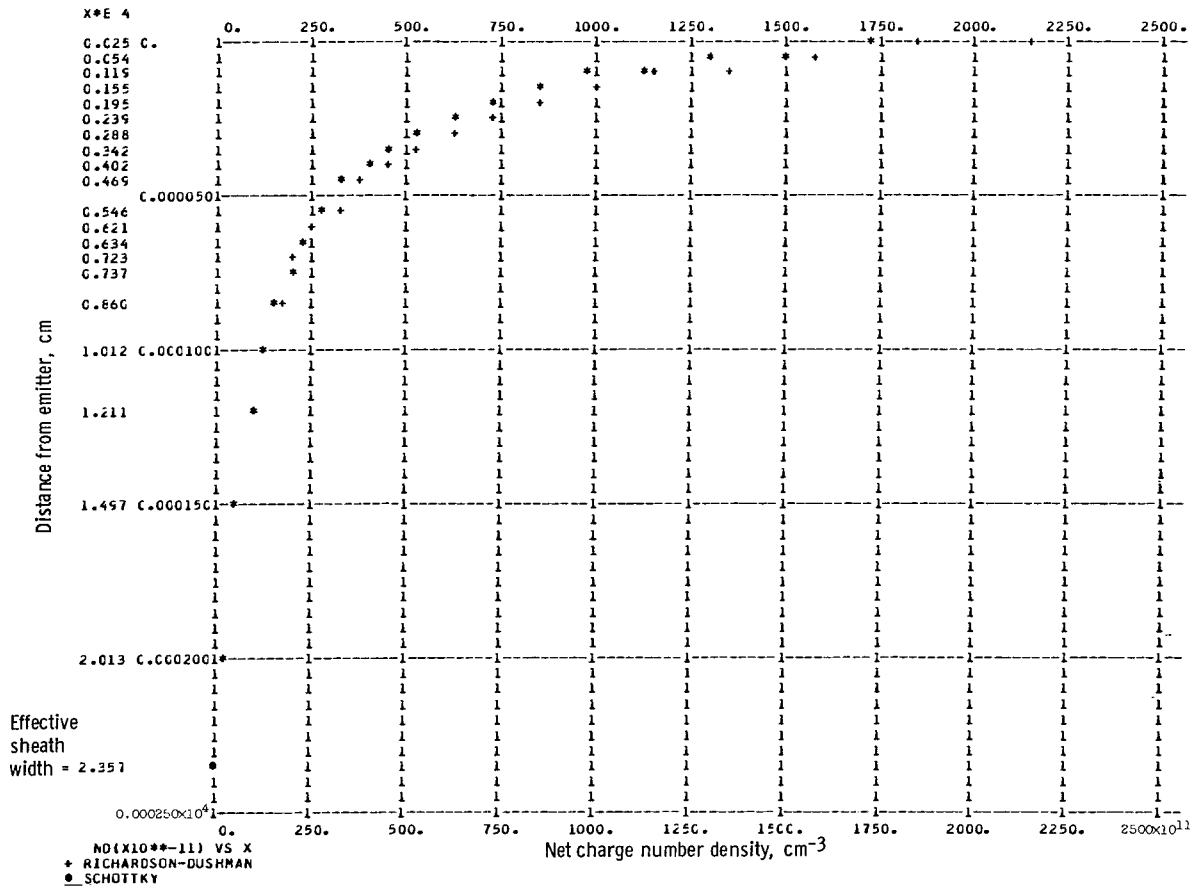

Figure 12. - Plane electron sheath between an emitter and a cesium plasma at equilibrium.

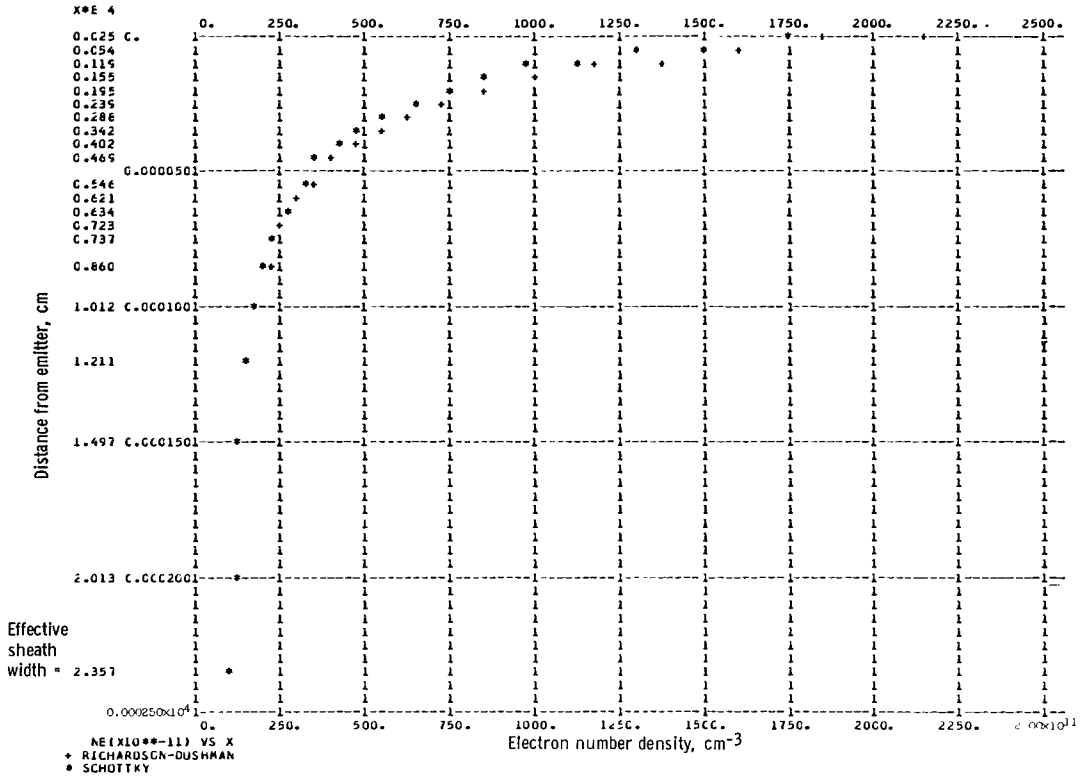

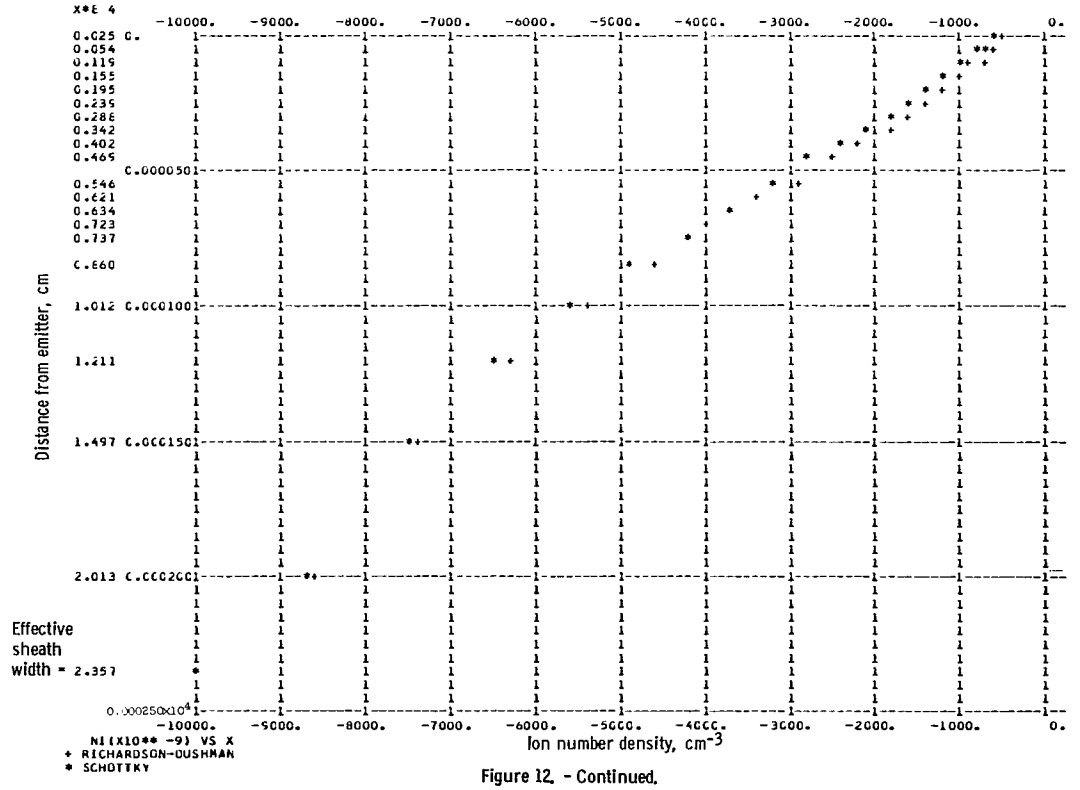

Figure 12. - Continued.

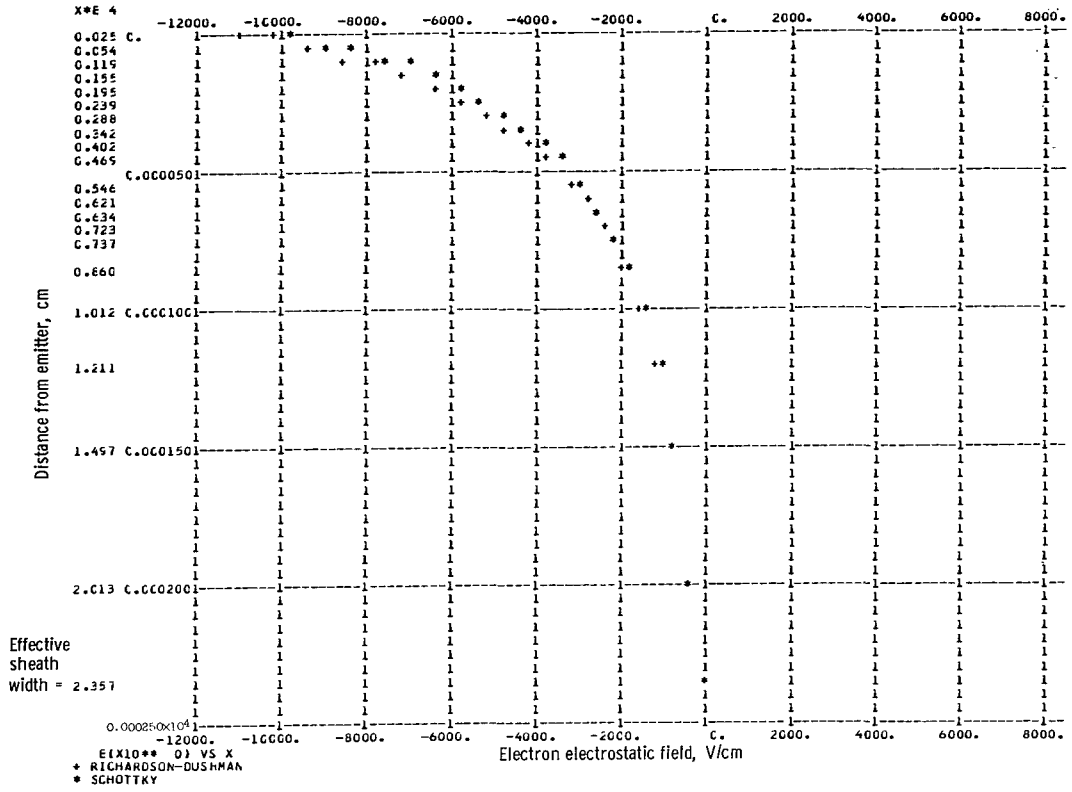

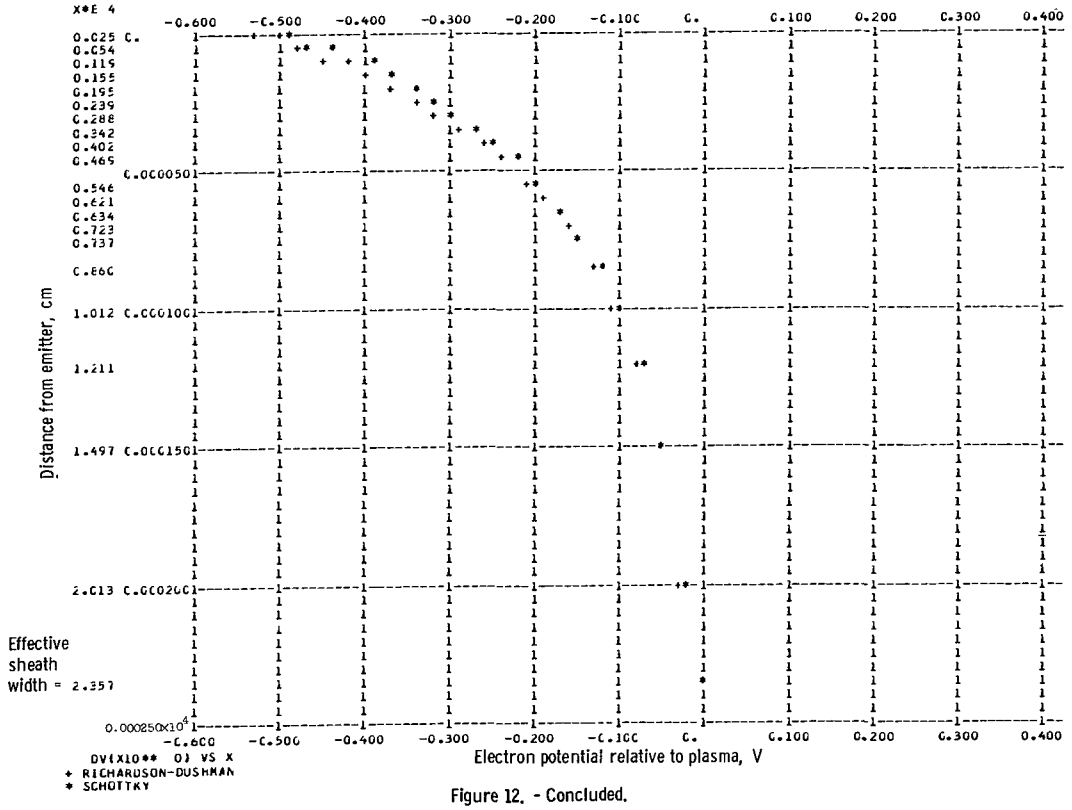

Figure 12. - Concluded.

SCHOTTKY

I = 3.893 TE = 2000. PHI = 2.500 NEP = 1.00E 13 TEP = 2200.0 TIP = 2000.0 LAMBDA = 1.0232E-04

PV = 8.283512E 04 LAMBDA(TE) = 5.7556E-05

DV	ND(DV)	NE(DV)	NI(DV)	E(DV)	X(DV)
0.	0.	1.000000E 13	-9.925125E 12	0.	2.326711E-04
-0.02461	2.596604E 12	1.158946E 13	-8.592858E 12	-3.655355E 02	1.950079E-04
-0.04522	5.929876E 12	1.336745E 13	-7.437573E 12	-7.291278E 02	1.484684E-04
-0.07383	8.576954E 12	1.541265E 13	-6.435692E 12	-1.093767E 03	1.203419E-04
-0.09544	1.220286E 13	1.776963E 13	-5.566772E 12	-1.463120E 03	1.006814E-04
-0.12305	1.567434E 13	2.048742E 13	-4.813084E 12	-1.839456E 03	8.558185E-05
-0.14766	1.946267E 13	2.362192E 13	-4.159253E 12	-2.224967E 03	7.336197E-05
-0.17227	2.364540E 13	2.723734E 13	-3.591944E 12	-2.621571E 03	6.313770E-05
-0.19688	2.830807E 13	3.140765E 13	-3.099585E 12	-3.031370E 03	5.438465E-05
-0.22149	3.354558E 13	3.621812E 13	-2.672133E 12	-3.456477E 03	4.676536E-05
-0.24610	3.946617E 13	4.176704E 13	-2.300865E 12	-3.899076E 03	4.004944E-05
-0.27071	4.618961E 13	4.816780E 13	-1.978196E 12	-4.361436E 03	3.407219E-05
-0.29532	5.385368E 13	5.555120E 13	-1.697519E 12	-4.845524E 03	2.871157E-05
-0.31993	6.261499E 13	6.406805E 13	-1.453064E 12	-5.355020E 03	2.387443E-05
-0.34454	7.265261E 13	7.389236E 13	-1.239756E 12	-5.891322E 03	1.948788E-05
-0.36915	8.417175E 13	8.522483E 13	-1.053086E 12	-6.457585E 03	1.549367E-05
-0.39376	9.740801E 13	9.829696E 13	-8.889495E 11	-7.056693E 03	1.184438E-05
-0.41837	1.126324E 14	1.133758E 14	-7.434035E 11	-7.691715E 03	8.500847E-06
-0.44298	1.301572E 14	1.307693E 14	-6.121295E 11	-8.365500E 03	5.430194E-06
-0.46759	1.503445E 14	1.508329E 14	-4.884453E 11	-9.082712E 03	2.604545E-06
-0.49221	1.736568E 14	1.739763E 14	-3.195106E 11	-9.845545E 03	0.

JEE	= 1.935250E 02	JEP	= 1.167033E 01	JIP	= 2.260730E-02	JAP	= 7.521643E-01
J	= -5.415518E-01	PP	= 7.325107E-02	JIE	= 1.445964E-04	JAE	= 7.533395E-01
JA	= 1.155272E-03	JI	= 1.155270E-03	JE	= -5.431070E-01	JAJAP	= 1.535690E-03
JE/JEP	= -4.653746E-02	JI/JIP	= 5.110163E-02	DVS	= -0.49221	XCVS	= 2.326711E-04
NAP	= 3.327175E 14	XDLAM	= 2.274013E 00	SC	= 3.766723E-02	PHZ	= 3.025?2
EDVS	= -9.845945E 03	DVSRD	= -5.257203E-01			DVS/RD	= 9.251751E-01
ELM/RD	= 1.901781E 00	PHZZ	= 3.025720E 00			DRD/KT	= 2.154266E 00
NTP	= 3.527175E 14	NCE	= 1.742959E 14	NTE	= 5.070133E 14	RE/KTE	= -3.073693E 00
X/LMTE	= 2.365005E 00	ELT/RD	= 1.813277E 00	NIPA	= -9.925125E 12		

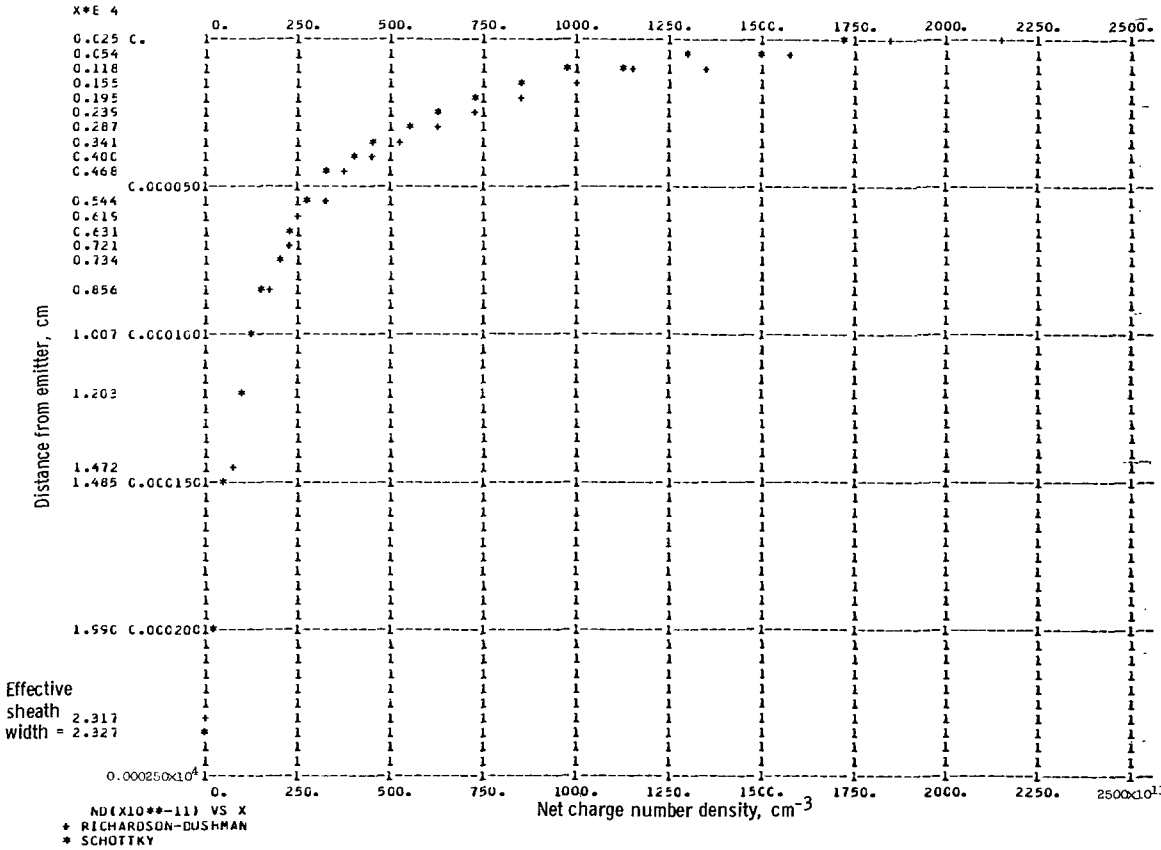

Figure 13. - Plane electron sheath between an emitter and a cesium plasma near equilibrium.

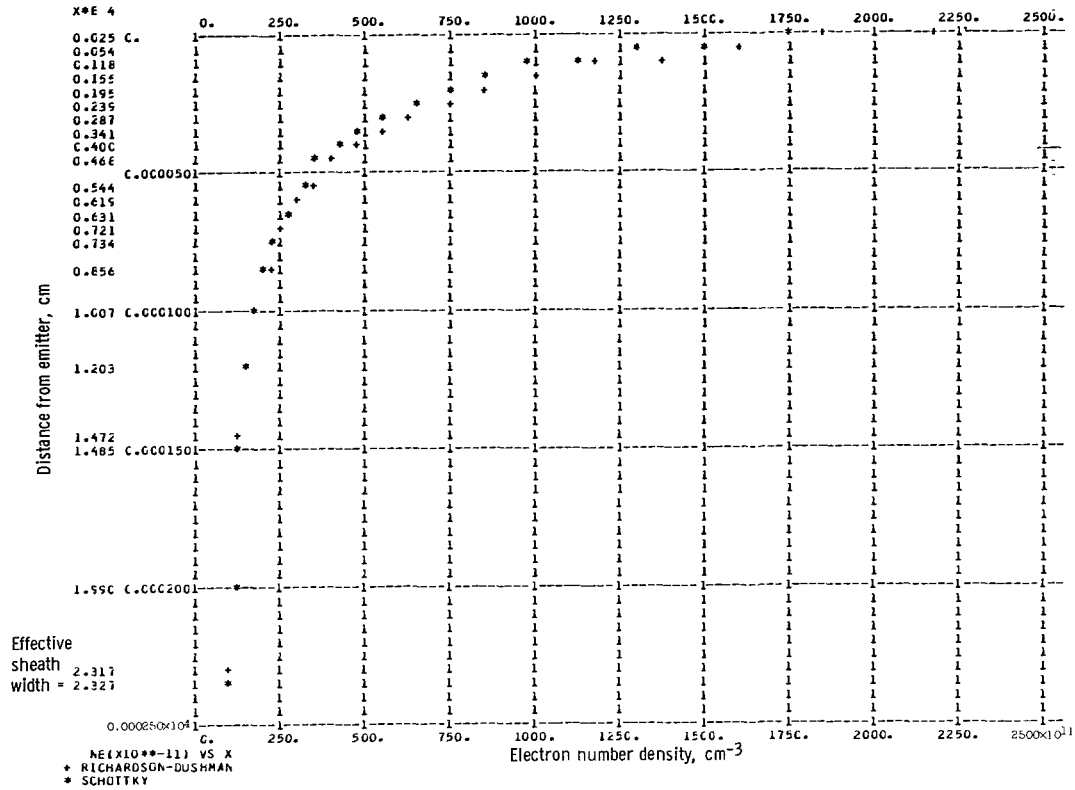

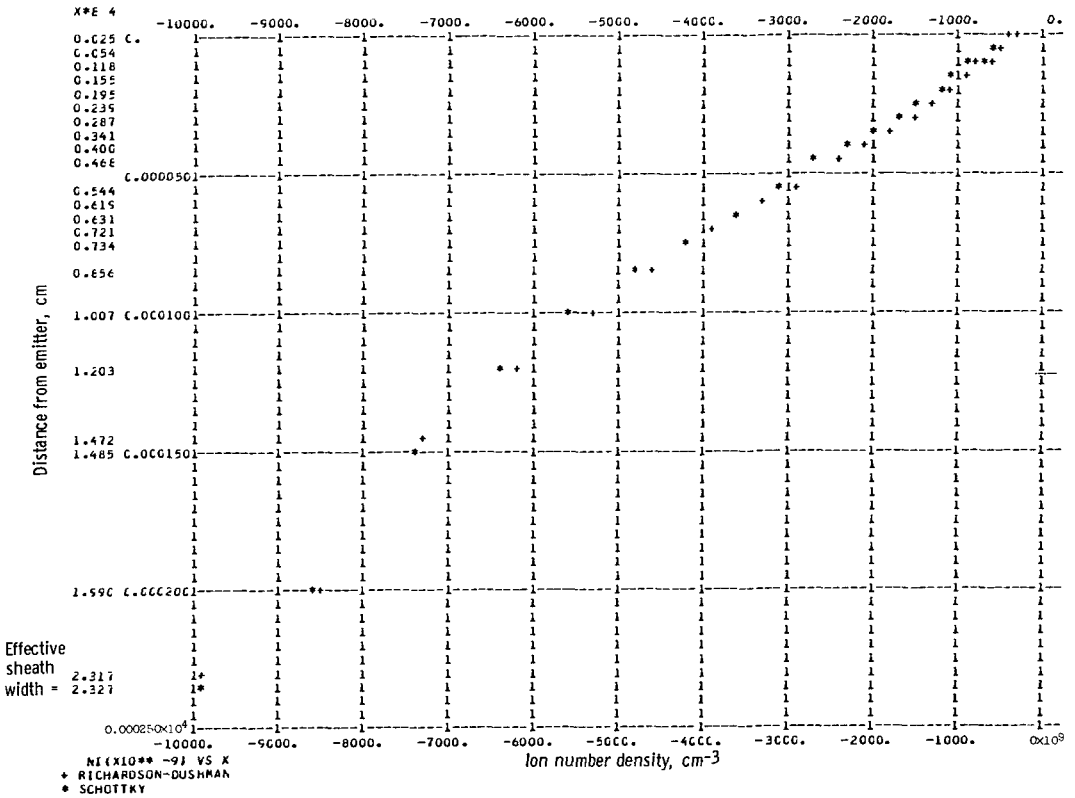

Figure 13. - Continued.

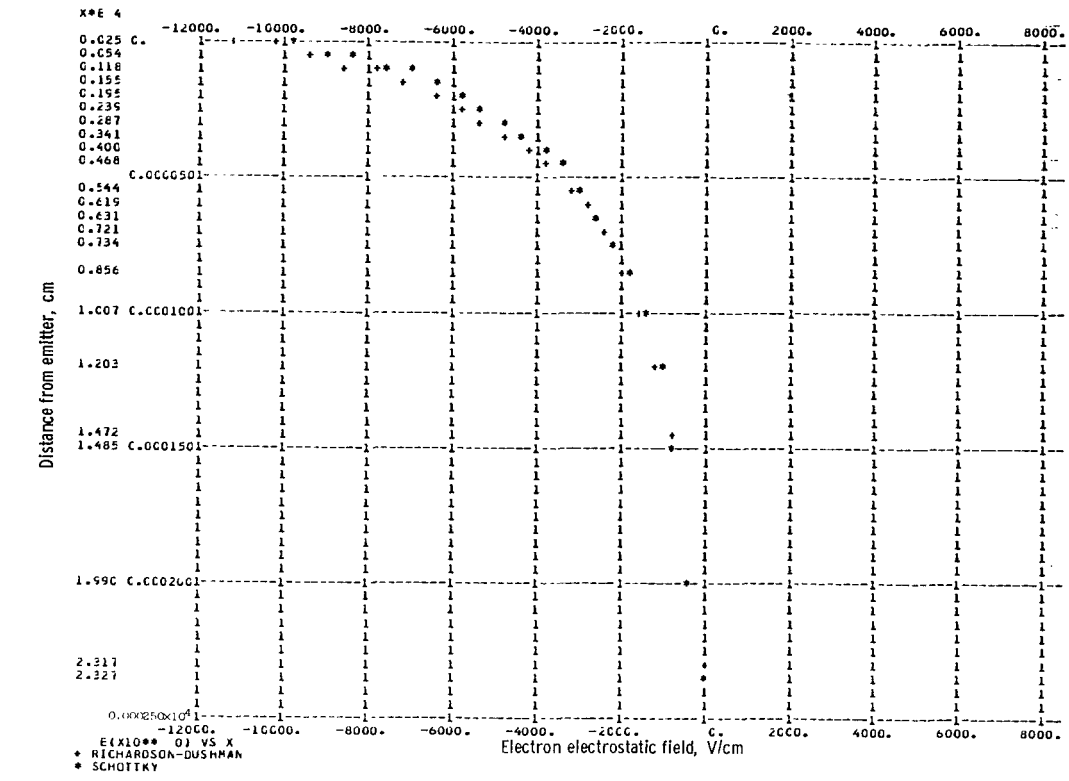

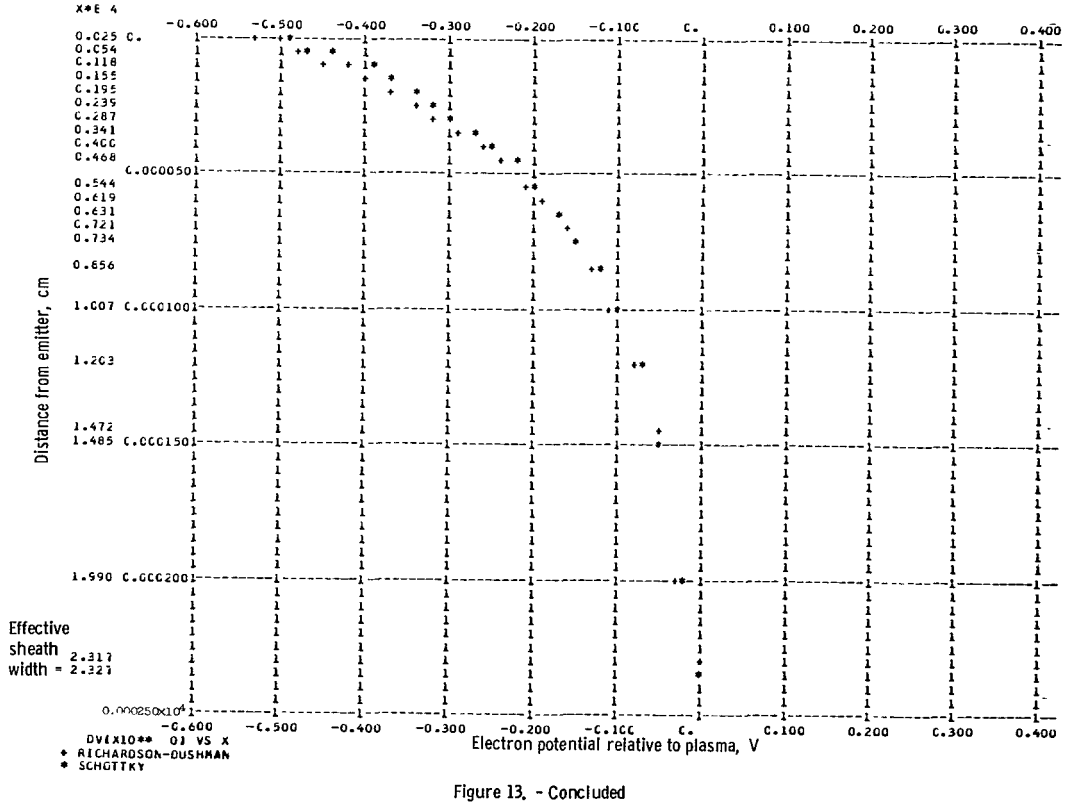

Figure 13. - Concluded

NATIONAL AERONAUTICS AND SPACE ADMINISTRATION
WASHINGTON, D. C. 20546
OFFICIAL BUSINESS

FIRST CLASS MAIL

POSTAGE AND FEES PAID
NATIONAL AERONAUTICS AND
SPACE ADMINISTRATION

07U 001 50 51 3DS 68226 00903
AIR FORCE WEAPONS LABORATORY/AFWL/
KIRTLAND AIR FORCE BASE, NEW MEXICO 87117

ATT E. LOU BOWMAN, ACTING CHIEF TECH. LIB

POSTMASTER: If Undeliverable (Section 158 Postal Manual) Do Not Return

"The aeronautical and space activities of the United States shall be conducted so as to contribute . . . to the expansion of human knowledge of phenomena in the atmosphere and space. The Administration shall provide for the widest practicable and appropriate dissemination of information concerning its activities and the results thereof."

—NATIONAL AERONAUTICS AND SPACE ACT OF 1958

NASA SCIENTIFIC AND TECHNICAL PUBLICATIONS

TECHNICAL REPORTS: Scientific and technical information considered important, complete, and a lasting contribution to existing knowledge.

TECHNICAL NOTES: Information less broad in scope but nevertheless of importance as a contribution to existing knowledge.

TECHNICAL MEMORANDUMS: Information receiving limited distribution because of preliminary data, security classification, or other reasons.

CONTRACTOR REPORTS: Scientific and technical information generated under a NASA contract or grant and considered an important contribution to existing knowledge.

TECHNICAL TRANSLATIONS: Information published in a foreign language considered to merit NASA distribution in English.

SPECIAL PUBLICATIONS: Information derived from or of value to NASA activities. Publications include conference proceedings, monographs, data compilations, handbooks, sourcebooks, and special bibliographies.

TECHNOLOGY UTILIZATION PUBLICATIONS: Information on technology used by NASA that may be of particular interest in commercial and other non-aerospace applications. Publications include Tech Briefs, Technology Utilization Reports and Notes, and Technology Surveys.

Details on the availability of these publications may be obtained from:

SCIENTIFIC AND TECHNICAL INFORMATION DIVISION

NATIONAL AERONAUTICS AND SPACE ADMINISTRATION

Washington, D.C. 20546